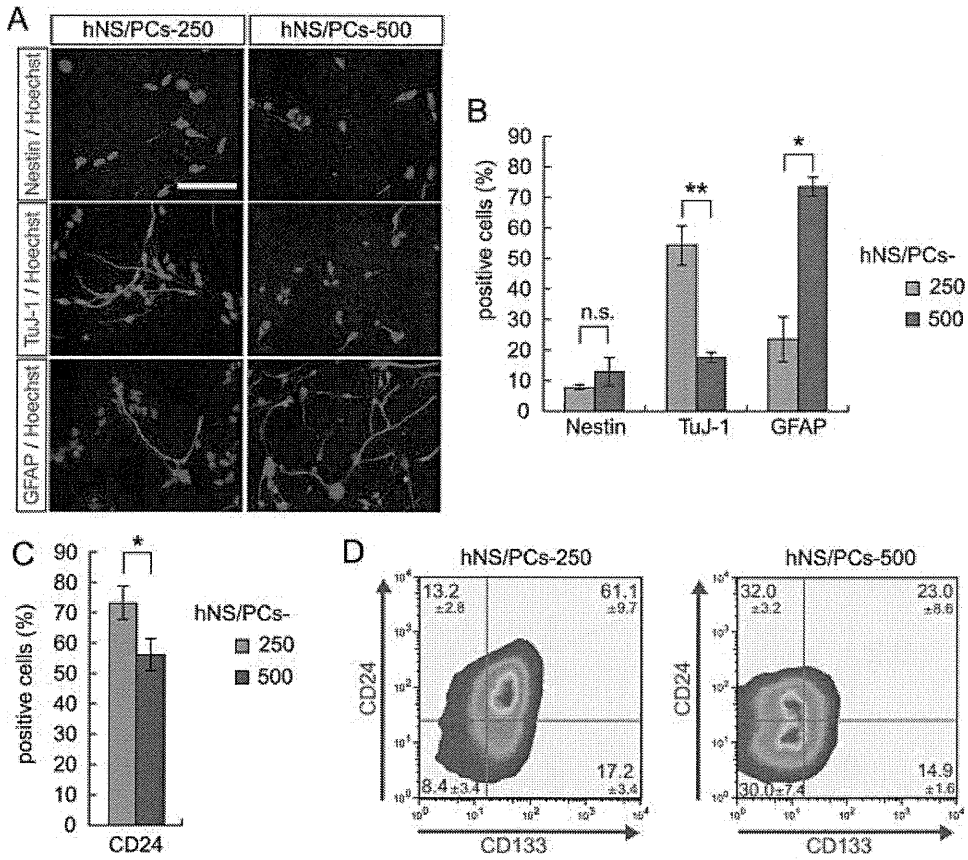

Fig. 2. Altered differentiation potentials between hNS/PCs-250 and -500. **A:** Immunocytochemical analysis of differentiated hNS/PCs for markers of neural progenitors (Nestin), neurons (TuJ-1), and astrocytes (GFAP). Quantitative analysis is shown in **B**. Only approximately 10% of the cells in both hNS/PCs-250 and -500 remained positive for Nestin. hNS/PCs-250 differentiated into significantly more TuJ-1-positive neurons than did hNS/PCs-500, whereas hNS/PCs-500 differentiated into significantly more GFAP-positive astrocytes than did hNS/PCs-250. **C:** Flow cytometric analysis of CD24, which is expressed in populations that include neuronal progenitors and postmitotic neurons. Consistent with the results in B, hNS/PCs-250 contained significantly more CD24-positive cells than did hNS/PCs-500. **D:** Coexpression of CD133 and CD24 by flow cytometric analysis. Consistently with the results in Figures 1 and 2B, hNS/PCs-250 contained significantly more $CD133^+$ cells and $CD24^+$ cells than did hNS/PCs-500; n = 3; means ± SEM. $*P < 0.05$; $**P < 0.01$; n.s., not significant ($P > 0.05$). Scale bar = 50 μm.

for transplantation therapy. For long-term observation, we used NOD/SCID mice, which are resistant to stress and infection and therefore show better survival than NOG mice. The results of the short-term experiment revealed that hNS/PCs-500 showed a lower proliferation ability than hNS/PCs-250 in vivo by Ki67 or PCNA immunostaining and a poor survival rate by BLI (only 3.8% 1 month after transplantation even in NOG mice) (Fig. 3A). Thus, for this long-term experiment, we monitored the in vivo tumorigenicity of only the hNS/PCs-250, as the better cell source for cell replacement therapy.

We transplanted hNS/PCs-250 into the right striatum of NOD/SCID mice and observed the survival of the grafted hNS/PCs by BLI for 6 months. The photon count of the luminescence generated by the surviving hNS/PCs was reduced to 12.8% ± 11.0% of the initial photon count at 8 weeks and thereafter maintained its signal for 6 months (10.0% ± 14.0%, n = 4; Fig. 5A). Notably, no rapid tumorigenic increase of the grafted hNS/PCs was observed within the 6 months following the transplantation. In contrast, control U87MG cells grew rapidly, showing a 419% increase in photon count 4 weeks after transplantation. Among the U87MG-transplanted mice, 75% (three of four) died by 5 weeks and the rest by 6 weeks after transplantation.

To examine the phenotype of the surviving cells derived from the transplanted hNS/PCs, we performed immunohistochemical analyses. Consistent with the findings of BLI, surviving Venus-positive cells were detected 3 months after transplantation (Fig. 5B). Most of them resided at the transplantation site for the entire 6 months and differentiated into TuJ-1-positive neurons and GFAP-positive astrocytes (Fig. 5C). In addition, Nestin-positive neural progenitors persisted even 6 months after the transplantation. However, the grafted hNS/PCs 6 months after transplantation in the long-term animals appeared to have larger nuclei and

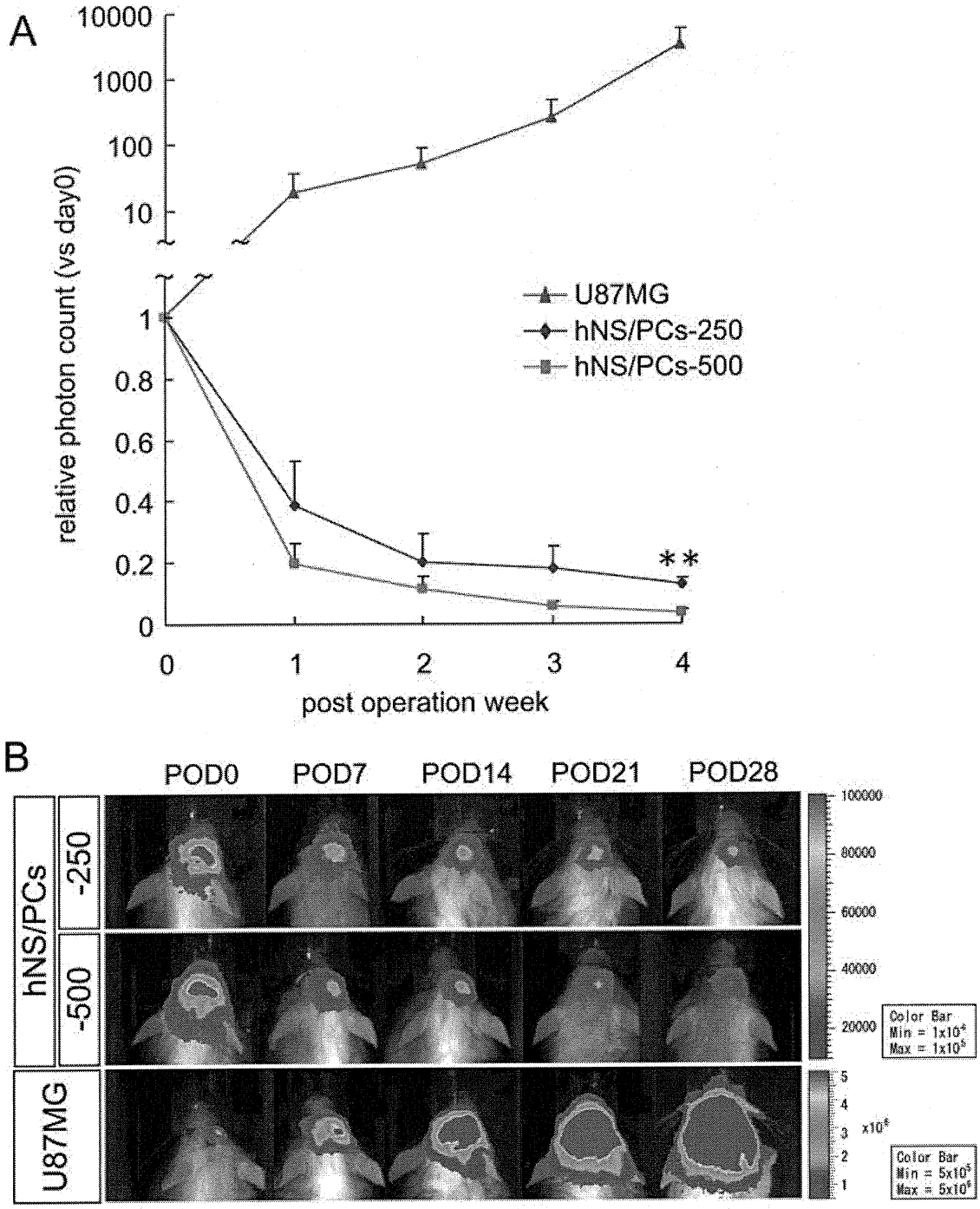

Fig. 3. Bioluminescence imaging of hNS/PCs-250 and -500 transplanted into NOG mice for up to 4 weeks. **A:** hNS/PCs-250, -500, and human glioblastoma cells (U87MG) were transplanted into the right striatum of NOG mice and observed by BLI for up to 4 weeks. hNS/PCs-250 exhibited significantly better survival and growth than did hNS/PCs-500 4 weeks after transplantation (n = 4; means ± SEM). $^{**}P < 0.01$. **B:** Representative BLI images of the treated mice.

lower cell densities than those observed 4 weeks after transplantation in the short-term animals (Fig. 5D). Importantly, we did not find any proliferating cells labeled by Ki67 or PCNA 6 months after transplantation (Fig. 5E) nor any obvious evidence of malignant invasive behavior by HE staining (Fig. 5F). Together

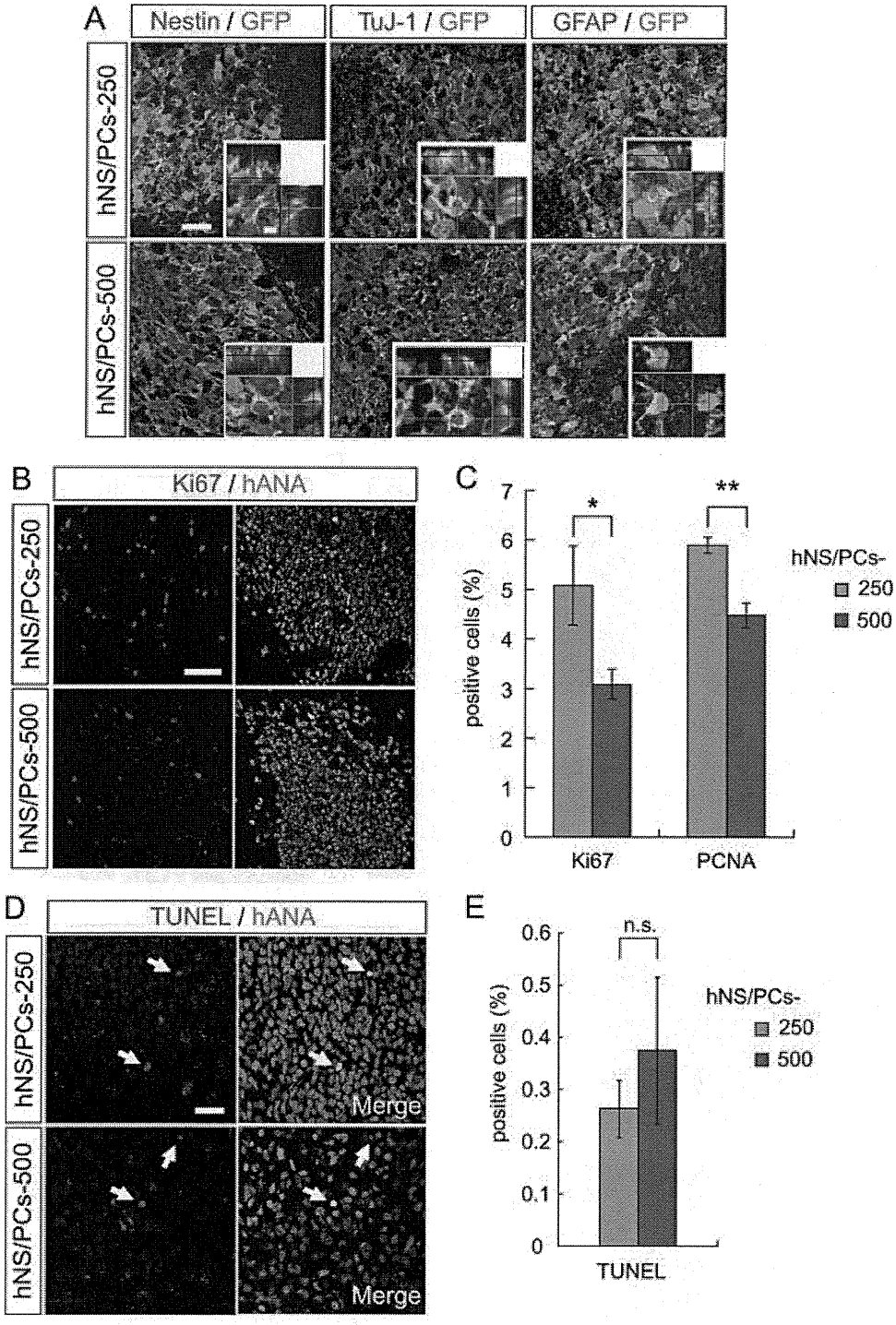

Fig. 4. Both hNS/PCs-250 and -500 appropriately differentiated into neurons and astrocytes in vivo. **A:** Immunofluorescence analysis of tissue sections 4 weeks after transplantation. Although some of the grafted hNS/PCs-250 and -500 still expressed Nestin, they had also differentiated into TuJ-1-positive neurons and GFAP-positive astrocytes. **B:** Representative image of Ki67-positive proliferating cells in the hNS/PCs-250 and -500 grafts. **C:** Quantitative analysis of the proportion of Ki67- and PCNA-positive cells in grafted hNS/PCs-250 and -500 4 weeks after transplantation. hNS/PCs-250 showed a significantly higher proportion of proliferating cells than did hNS/PCs-500. **D:** Analysis of apoptotic cells by TUNEL staining in grafted hNS/PCs. **E:** Quantitative analysis of TUNEL-positive cells. No significant difference in the TUNEL-positive apoptotic cells was observed between hNS/PCs-250 and -500. All data are presented as the mean ± SEM; n = 3. $*P < 0.05$; $**P < 0.01$; n.s., not significant. Scale bars = 20 μm and 5 μm for low- and high-magnification images, respectively, in A; 50 μm in B; 20 μm in D.

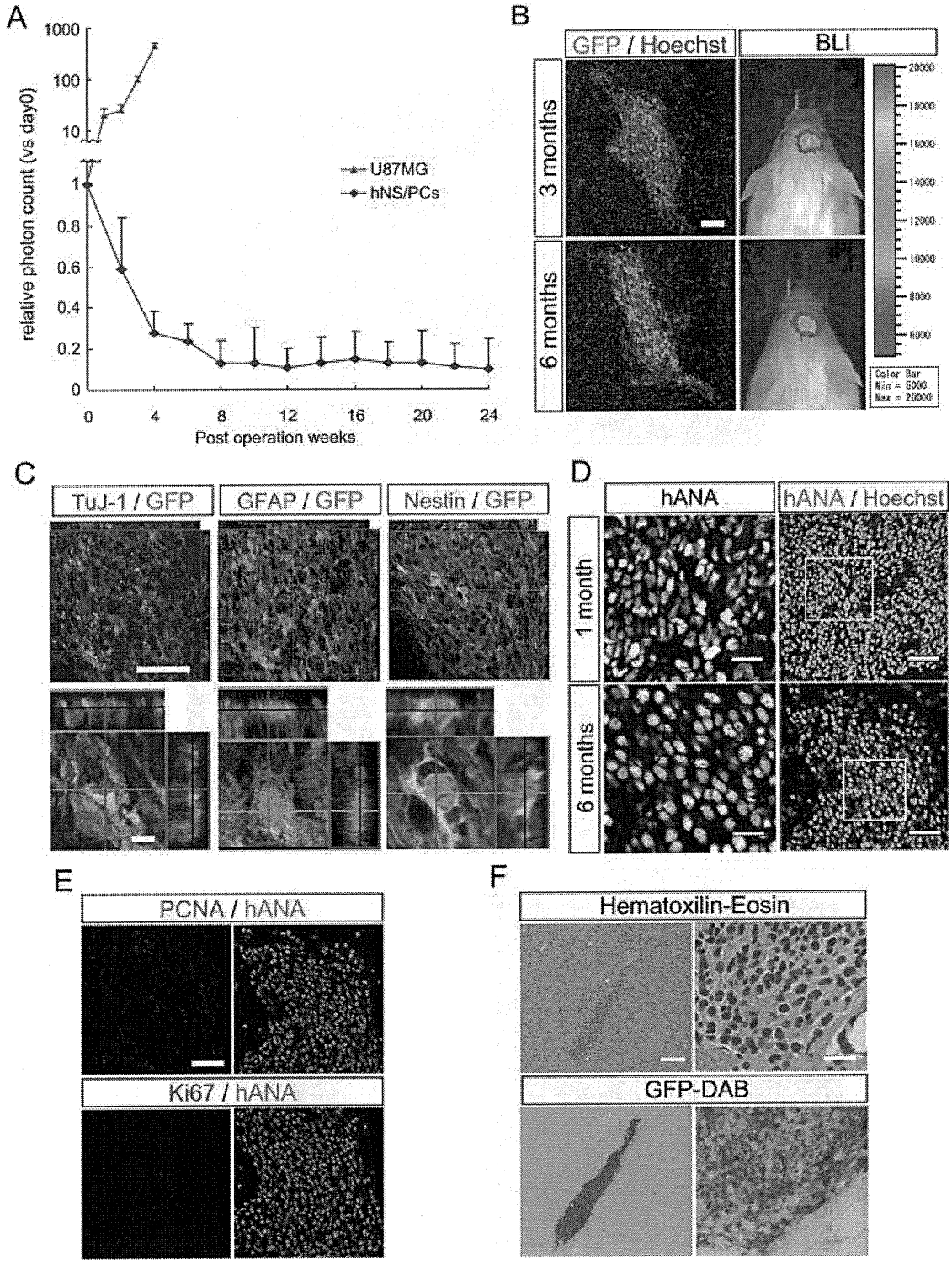

Fig. 5. hNS/PCs did not exhibit tumorigenesis for 6 months. **A:** Long-term observation of grafted hNS/PCs-250 by BLI for 6 months. The photon count of hNS/PCs decreased for 8 weeks after transplantation but was stable thereafter. The hNS/PCs did not show any evidence of tumorigenicity during the 6-month observation period, unlike the control U87MG cells. Data are presented as the mean ± SEM. **B:** Immunohistochemical analysis of Venus-expressing grafted hNS/PCs 3 and 6 months after transplantation showed consistent correlation of the Venus-expressing area with the photon counts detected by BLI. **C:** Immunohistochemical analysis of grafted hNS/PCs 6 months after transplantation. hNS/PCs resided at the site of injection and differentiated into TuJ-1-positive neurons and GFAP-positive astrocytes. However, Nestin-positive neural progenitors were also observed, even 6 months after transplantation. **D:** hANA and Hoechst nuclear staining of the grafted area 1 month and 6 months after the transplantation. Grafted cells showed larger nuclei and lower cell densities in the long-term analysis than in the short-term analysis. **E:** Immunohistochemical analysis of proliferation markers PCNA and Ki67. Neither PCNA- nor Ki67-positive cells were observed. **F:** Hematoxylin-eosin and GFP-DAB staining indicated no malignant invasive features in the transplanted cells. Scale bars = 100 μm in B; low-magnification image 50 μm, high-magnification image 5 μm in C; low-magnification image 50 μm, high-magnification image 20 μm in D; 50 μm in E; low-magnification image 200 μm, high-magnification image 20 μm in F.

these findings indicate that the grafted hNS/PCs could survive and differentiate properly in the brain of NOD/SCID mice without any tumor formation, at least for 6 months after transplantation.

DISCUSSION

Human Fetal Neurospheres Exhibited Altered Proliferation and Differentiation Properties In Vitro and In Vivo, Depending on the Culture Period

Because large numbers of human fetus-derived cells are difficult to obtain unless they are expanded in vitro, it is essential to evaluate the differentiation and proliferation properties as well as tumorigenic potential of in-vitro-expanded hNS/PCs when considering their clinical use in cell replacement therapies. In the present study, we clearly showed the likely senescence of hNS/PCs maintained for more than 500 DIV, from their differentiation and proliferation properties. More importantly, we also showed the lack of tumorigenicity of hNS/PCs-250 over the long term in vivo. This is the first report in which the in vivo tumorigenicity of transplanted in-vitro-maintained hNS/PCs was evaluated by long-term monitoring with BLI.

The in vitro ATP assay (Fig. 1A) and in vivo BLI study (Fig. 3A) showed that hNS/PCs-250 had significantly higher growth and survival rates than did hNS/PCs-500 both in vitro and in vivo. This difference between hNS/PCs-250 and -500 in vitro was attributable to a reduced proportion of dividing cells in the hNS/PCs-500, shown by positive staining for Ki67 or PCNA, or in the cell cycle of S/G2/M, but not to the proportion of annexin V-positive apoptotic cells. In addition, the proportion of $CD133^+$ undifferentiated hNS/PCs was lower in the older hNS/PCs-500 than in the younger hNS/PCs-250. Thus, hNS/PCs seem to lose their ability to self-renew and acquire the properties of committed progenitors or postmitotic cells during their long-term culture in vitro.

Interestingly, this difference in self-renewability between hNS/PCs-250 and -500 seemed to be correlated with an alteration in their differentiation potentials. hNS/PCs-250 exhibited more neurogenic and fewer gliogenic properties than hNS/PCs-500 (Fig. 2A,B). Given that the $CD24^+$ cells are proposed to be associated with the population of committed neuronal progenitors and neurons (Calaora et al., 1996; Shewan et al., 1996; Doetsch et al., 1999; Murayama et al., 2002; Nieoullon et al., 2005; Pruszak et al., 2007), the significantly higher proportion of $CD24^+$ cells in hNS/PCs-250 than in hNS/PCs-500 (Fig. 2C,D) also supports the idea that the hNS/PCs-250 contain more neurogenic progenitors than do the hNS/PCs-500, which contain more gliogenic progenitors. Taken together, these findings suggest that human fetal neurospheres lose multipotent and self-renewable hNS/PCs, which are replaced by progenitors committed to become glial cells, after long-term maintenance in vitro.

Long-Term Observation by BLI Revealed hNS/PCs To Be Nontumorigenic up to 6 Months After Their Transplantation Into NOD/SCID Striatum

Although some reports have examined the safety of grafted cells, including their long-term potential for tumorigenicity, by histological analyses, this type of analysis does not allow the dynamics of donor cells to be observed over time in the same live animal. In the present study, we monitored the survival of hNS/PCs grafted into the NOD/SCID striatum by BLI. Because we do not have to sacrifice the animals at each time point for histological analysis, we can repeatedly examine the same grafted animal and sequentially evaluate the in vivo tumorigenicity of the donor cells. This monitoring system allows a more accurate analysis than the conventional intermittent histological method.

The findings that the photon counts of engrafted hNS/PCs-250 decreased to 12.8% of the initial count within 8 weeks after transplantation and that their signals were maintained thereafter for up to 6 months without any tumorigenic proliferation, unlike the U87MG glioblastoma cell line, suggested that hNS/PCs-250 are not tumorigenic. These results were confirmed by histological analyses. The Venus-positive area 6 months after transplantation was no greater than the area 3 months after the surgery. No Ki67- or PCNA-positive proliferative cells were observed 6 months after the transplantation. HE staining indicated a pathology that lacked any malignant invasive behavior. Taken together, these results strongly indicate that the hNS/PCs-250 were negative for tumorigenicity. Surprisingly, the Venus-positive grafted cells were still positive for Nestin even 6 months after the transplantation, but they were negative for the proliferation markers Ki67 and PCNA (Fig. 5E). Moreover, the density of the grafted cells was much lower in animals 6 months after grafting than 1 month after grafting (Fig. 5D). Although we cannot clarify the properties of these Nestin-positive but proliferation marker-negative cells, they might reside in the grafted sites as dormant neural stem cells. Therefore, further evaluation of the safety of these donor cells, such as observation periods much longer than 6 months, is warranted.

In conclusion, we showed that the maintenance and safety of transplanted hNS/PCs could be assessed by monitoring the dynamics of these cells in vivo using BLI. Our present study provides a reliable system for evaluating the tumorigenicity of hNS/PCs in vivo and addresses several issues that are prerequisites for the clinical application of hNS/PCs, including defining their properties in vitro and in vivo and their tumorigenicity when transplanted after long-term maintenance in culture. Taken together with previous reports, our data indicate that the prospect for the future application of hNS/PCs to cell replacement therapies for neurological disorders is very promising.

ACKNOWLEDGMENTS

We are grateful to Dr. S. Mitani for the anti-GFP antibody; Drs. T. Nomura and K. Tamaoki for the NOG mice; Dr. M. Yamasaki for the human neural

stem/progenitor cells; Dr. H. Miyoshi for the lenti-virus vector; Dr. Y. Toyama for continuous encouragement; Mrs. Y. Yamashita, Ms. A. Yokokawa, and Mrs. T. Harada for technical assistance; and all the members of Dr. Okano's laboratory for encouragement and kind support.

REFERENCES

Anderson L, Burnstein RM, He X, Luce R, Furlong R, Foltynie T, Sykacek P, Menon DK, Caldwell MA. 2007. Gene expression changes in long term expanded human neural progenitor cells passaged by chopping lead to loss of neurogenic potential in vivo. Exp Neurol 204:512–524.

Barraud P, Stott S, Mollgard K, Parmar M, Anders B. 2007. In vitro characterization of a human neural progenitor cell coexpressing SSEA4 and CD133. J Neurosci Res 85:250–259.

Calaora V, Chazal G, Nielsen PJ, Rougon G, Moreau H. 1996. mCD24 expression in the developing mouse brain and in zones of secondary neurogenesis in the adult. Neuroscience 73:581–594.

Caldwell MA, He X, Wilkie N, Pollack S, Marshall G, Wafford KA, Svendsen CN. 2001. Growth factors regulate the survival and fate of cells derived from human neurospheres. Nat Biotechnol 19:475–479.

Carpenter MK, Cui X, Hu Z, Jackson J, Sherman S, Seiger A, Wahlberg LU. 1999. In vitro expansion of a multipotent population of human neural progenitor cells. Exp Neurol 158:265–278.

Crouch SPM, Kozlowski R, Slater KJ, Fletcher J. 1993. The use of ATP bioluminescence as a measure of cell proliferation and cytotoxicity. J Immunol Methods 160:81–88.

Cummings BJ, Uchida N, Tamaki SJ, Salazar DL, Hooshmand M, Summers R, Gage FH, Anderson AJ. 2005. Human neural stem cells differentiate and promote locomotor recovery in spinal cord-injured mice. Proc Natl Acad Sci U S A 102:14069–14074.

Deitch A, Law H, deVere White R. 1982. A stable propidium iodide staining procedure for flow cytometry. J Histochem Cytochem 30:967–972.

Doetsch F, Caille I, Lim DA, Garcia-Verdugo JM, Alvarez-Buylla A. 1999. Subventricular zone astrocytes are neural stem cells in the adult mammalian brain. Cell 97:703–716.

Ito M, Hiramatsu H, Kobayashi K, Suzue K, Kawahata M, Hioki K, Ueyama Y, Koyanagi Y, Sugamura K, Tsuji K, Heike T, Nakahata T. 2002. NOD/SCID/gamma cnull mouse: an excellent recipient mouse model for engraftment of human cells. Blood 100:3175–3182.

Iwanami A, Kaneko S, Nakamura M, Kanemura Y, Mori H, Kobayashi S, Yamasaki M, Momoshima S, Ishii H, Ando K, Tanioka Y, Tamaoki N, Nomura T, Toyama Y, Okano H. 2005. Transplantation of human neural stem cells for spinal cord injury in primates. J Neurosci Res 80:182–190.

Jeong S, Chu K, Jung K, Kim SU, Kim M, Roh J-K. 2003. Human neural stem cell transplantation promotes functional recovery in rats with experimental intracerebral hemorrhage. Stroke 34:2258–2263.

Kanemura Y, Mori H, Kobayashi S, Islam O, Kodama E, Yamamoto A, Nakanishi Y, Arita N, Yamasaki M, Okano H, Hara M, Miyake J. 2002. Evaluation of in vitro proliferative activity of human fetal neural stem/progenitor cells using indirect measurements of viable cells based on cellular metabolic activity. J Neurosci Res 69:869–879.

Keyoung HM, Roy NS, Benraiss A, Louissaint A, Suzuki A, Hashimoto M, Rashbaum WK, Okano H, Goldman SA. 2001. High-yield selection and extraction of two promoter-defined phenotypes of neural stem cells from the fetal human brain. Nat Biotechnol 19:843–850.

Masuda H, Maruyama T, Hiratsu E, Yamane J, Iwanami A, Nagashima T, Ono M, Miyoshi H, Okano HJ, Ito M, Tamaoki N, Nomura T, Okano H, Matsuzaki Y, Yoshimura Y. 2007. Noninvasive and real-time assessment of reconstructed functional human endometrium in NOD/SCID/γ-formula immunodeficient mice. Proc Natl Acad Sci U S A 104:1925–1930.

McBride JL, Behrstock SP, Chen E, Jakel RJ, Irwin Siegel CNS, Kordower JH. 2004. Human neural stem cell transplants improve motor function in a rat model of Huntington's disease. J Comp Neurol 475:211–219.

Miyoshi H, Blomer U, Takahashi M, Gage FH. 1998. Development of a self-inactivating lentivirus vector. J Virol 72:8150–8157.

Murayama A, Matsuzaki Y, Kawaguchi A, Shimazaki T, Okano H. 2002. Flow cytometric analysis of neural stem cells in the developing and adult mouse brain. J Neurosci Res 69:837–847.

Nakamura Y, Yamamoto M, Oda E, Yamamoto A, Kanemura Y, Hara M, Suzuki A, Yamasaki M, Okano H. 2003. Expression of tubulin beta II in neural stem/progenitor cells and radial fibers during human fetal brain development. Lab Invest 83:479–489.

Nieoullon V, Belvindrah R, Rougon G, Chazal G. 2005. mCD24 regulates proliferation of neuronal committed precursors in the subventricular zone. Mol Cell Neurosci 28:462–474.

Okada S, Ishii K, Yamane J, Iwanami A, Ikegami T, Katoh H, Iwamoto Y, Nakamura M, Miyoshi H, Okano HJ, Contag CH, Toyama Y, Okano H. 2005. In vivo imaging of engrafted neural stem cells: its application in evaluating the optimal timing of transplantation for spinal cord injury. FASEB J 19:1839–1841.

Okano H. 2002. Stem cell biology of the central nervous system. J Neurosci Res 69:698–707.

Panchision DM, Chen H-L, Pistollato F, Papini D, Ni H-T, Hawley TS. 2007. Optimized flow cytometric analysis of central nervous system tissue reveals novel functional relationships among cells expressing CD133, CD15, and CD24. Stem Cells 25:1560–1570.

Petty RD, Sutherland LA, Hunter EM, Cree IA. 1995. Comparison of MTT and ATP-based assays for the measurement of viable cell number. J Biolumin Chemilumin 10:29–34.

Piao J, Odeberg J, Samuelsson EB, Kjaeldgaard A, Falci S, Seiger A, Sundstrom E, Akesson E. 2006. Cellular composition of long-term human spinal cord- and forebrain-derived neurosphere cultures. J Neurosci Res 84:471–482.

Pruszak J, Sonntag KC, Aung MH, Sanchez-Pernaute R, Isacson O. 2007. Markers and methods for cell sorting of human embryonic stem cell-derived neural cell populations. Stem Cells 25:2257–2268.

Reynolds B, Weiss S. 1992. Generation of neurons and astrocytes from isolated cells of the adult mammalian central nervous system. Science 255:1707–1710.

Shewan D, Calaora V, Nielsen P, Cohen J, Rougon G, Moreau H. 1996. mCD24, a glycoprotein transiently expressed by neurons, is an inhibitor of neurite outgrowth. J Neurosci 16:2624–2634.

Shultz L, Schweitzer P, Christianson S, Gott B, Schweitzer I, Tennent B, McKenna S, Mobraaten L, Rajan T, Greiner D. 1995. Multiple defects in innate and adaptive immunologic function in NOD/LtSz-scid mice. J Immunol 154:180–191.

Svendsen CN, ter Borg MG, Armstrong RJE, Rosser AE, Chandran S, Ostenfeld T, Caldwell MA. 1998. A new method for the rapid and long term growth of human neural precursor cells. J Neurosci Methods 85:141–152.

Uchida N, Buck DW, He D, Reitsma MJ, Masek M, Phan TV, Tsukamoto AS, Gage FH, Weissman IL. 2000. Direct isolation of human central nervous system stem cells. Proc Natl Acad Sci U S A 97:14720–14725.

Vescovi AL, Parati EA, Gritti A, Poulin P, Ferrario M, Wanke E, Frolichsthal-Schoeller P, Cova L, Arcellana-Panlilio M, Colombo A, Galli R. 1999. Isolation and cloning of multipotential stem cells from the embryonic human CNS and establishment of transplantable human neural stem cell lines by epigenetic stimulation. Exp Neurol 156:71–83.

Wright LS, Prowse KR, Wallace K, Linskens MHK, Svendsen CN. 2006. Human progenitor cells isolated from the developing cortex undergo decreased neurogenesis and eventual senescence following expansion in vitro. Exp Cell Res 312:2107–2120.

Neuroscience Research 65 (2009) 384–392

Contents lists available at ScienceDirect

Neuroscience Research

journal homepage: www.elsevier.com/locate/neures

Transplantation of dendritic cells promotes functional recovery from spinal cord injury in common marmoset

Masae Yaguchi [a], Masanao Tabuse [b], Shigeki Ohta [a], Kozo Ohkusu-Tsukada [a], Tamaki Takeuchi [a], Junichi Yamane [c], Hiroyuki Katoh [c], Masaya Nakamura [c], Yumi Matsuzaki [d], Masayuki Yamada [e,f], Toshio Itoh [f], Tatsuji Nomura [f], Yoshiaki Toyama [c], Hideyuki Okano [d], Masahiro Toda [a,b,*]

[a] *Neuroimmunology Research Group, Keio University School of Medicine, Tokyo, Japan*
[b] *Department of Neurosurgery, Keio University School of Medicine, Tokyo, Japan*
[c] *Department of Orthopaedic Surgery, Keio University School of Medicine, Tokyo, Japan*
[d] *Department of Physiology, Keio University School of Medicine, Tokyo, Japan*
[e] *Faculty of Radiological Technology, Fujita Health University, School of Health Sciences, Aichi, Japan*
[f] *Central Institute for Experimental Animals, Kawasaki, Kanagawa, Japan*

ARTICLE INFO

Article history:
Received 12 February 2009
Received in revised form 21 August 2009
Accepted 31 August 2009
Available online 6 September 2009

Keywords:
Dendritic cells
Spinal cord injury
Non-human primate
Transplantation

ABSTRACT

We previously reported that implantation of dendritic cells (DCs) into the injured site activates neural stem/progenitor cells (NSPCs) and promotes functional recovery after spinal cord injury (SCI) in mice. Working toward clinical application of DC therapy for SCI, we analyzed whether DCs promote functional recovery after SCI in a non-human primate, the common marmoset (CM). CMs are usually born as dizygotic twins. They are thus natural bone marrow and peripheral blood chimeras due to sharing of the placental circulation between dizygotic twins, leading to functional immune tolerance. In this study, to identify adequate CM donor-and-host pairs, mixed leukocyte reaction (MLR) assays were performed. Then, CM-DCs were generated from the bone marrow of the twin selected to be donor and transplanted into the injured site of the spinal cord of the other twin selected to be host, 7 days after injury. Histological analyses revealed fewer areas of demyelination around the injured site in DC-treated CMs than in controls. Immunohistochemical analysis showed that more motor neurons and corticospinal tracts were preserved after SCI in DC-treated CMs. Motor functions were evaluated using three different behavior tests and earlier functional recovery was observed in DC-treated CMs. These results suggest DC therapy to possibly be beneficial in primates with SCI and that this treatment has potential for clinical application.

1. Introduction

Because repair is very limited after central nervous system (CNS) injury, especially in spinal cord injury (SCI), the development of new therapies is urgently needed for CNS injury. Recently, various cell therapies have been studied for the treatment of SCI using ES cells (McDonald et al., 1999), neural stem cells (Cummings et al., 2005; Ogawa et al., 2002, Okano, 2002), bone marrow cells (Koda et al., 2005; Koshizuka et al., 2004), Schwann cells (Martin et al., 1996; Takami et al., 2002), and olfactory ensheathing cells (Doucette, 1995; Richter and Roskams, 2008) in animal models. Immune-cell-based therapy using T cells and macrophages has also been reported for the treatment of SCI (Hauben et al., 2000). Most interestingly, activated macrophages showed a beneficial effect in a human clinical study (Knoller et al., 2005).

Dendritic cells (DCs), which are antigen presentation cells (APCs), have the ability to prime T cells for immune responses against viruses, bacteria and tumors. Immature DCs can capture and process exogenous antigens, and following maturation, migrate to lymphoid organs, where they stimulate potent antigen-specific T cells (Steinman, 1991; Steinman et al., 2003). Based on their strong ability to activate cytotoxic T lymphocytes, DCs are regarded as a useful tool for cancer immunotherapy and are currently being used in human clinical studies for the treatment of various cancers (Banchereau and Palucka, 2005; Nencioni and Brossart, 2004; Schuler et al., 2003). Recently, we reported that implantation of DCs into the injured site of the mouse spinal cord produced functional recovery with *de-novo* neurogenesis (Mikami et al., 2004). Murine DCs were shown to secrete NT-3 and activate neural stem/progenitor cells (NSPCs).

* Corresponding author at: Department of Neurosurgery, Keio University School of Medicine, 35 Shinanomachi, Shinjuku-ku, Tokyo 160-8582, Japan. Tel.: +81 3 5363 3587.
E-mail address: todam@sc.itc.keio.ac.jp (M. Toda).

0168-0102/$ – see front matter © 2009 Elsevier Ireland Ltd and the Japan Neuroscience Society. All rights reserved.
doi:10.1016/j.neures.2009.08.016

Working toward the clinical application of novel therapies, studies using non-human primates are valuable for ensuring both the therapeutic effects and safety (Courtine et al., 2007). Compared with other monkeys, the common marmoset (*Callithrix jacchus*; CM) offers many advantages for preclinical studies (Abbott et al., 2003; Ludlage and Mansfield, 2003; Mansfield, 2003). The average weight of an adult CM is 200–300 g, and adult body length (without tail) is 14–19 cm, making it possible to handle and breed these animals easily on a large scale and thereby reduce the cost of experiments (Ludlage and Mansfield, 2003). CMs have been used in studies on CNS diseases including Parkinson's disease (Gnanalingham et al., 1993), stroke (Marshall et al., 2000), Huntington's disease (Kendall et al., 1998), multiple sclerosis (t Hart et al., 1998, 2004), anxiety (Barros et al., 2000) and SCI (Fouad et al., 2004; Iwanami et al., 2005b; Liu et al., 2001). We recently established culture methods for DCs in CMs (Ohta et al., 2008). With the goal of clinical application of DC therapy, in this study, we analyzed the effects, safety, and feasibility of this therapy in a SCI model of CM.

2. Materials and methods

2.1. Animals and spinal cord injury

Adult CM (260–400 g; 1–2 years old, Clea Japan Inc., Tokyo, Japan) were used in this study. Contusive SCIs were induced using a weight-drop device (a modified NYU impactor with a diameter of 3.5 mm) as described previously (Iwanami et al., 2005a). After an intramuscular injection of ketamine (50 mg/kg) and xylazine (5 mg/kg) to induce anesthesia, a C5 laminectomy was carried out and a 17 g weight was dropped from a height of 50 mm onto the exposed dura matter (Iwanami et al., 2005a). A week after injury, $4–8 \times 10^6$ DCs in 10–15 μl of RPMI medium (Sigma, St. Louis, MO) or RPMI-1640 medium (10–15 μl) were injected into the center of the lesion site using a micro-stereotaxic injection system (David Kopf Instruments, Tujunga, CA). All animals received daily ampicillin (100 mg/kg intramuscularly; Meiji Seika Kaisha, Ltd., Tokyo, Japan) for 1 week after injury. The ethics committee of the institute approved all surgical interventions and animal care procedures, which were carried out in accordance with the Laboratory Animal Welfare Act, the Guide for the Care and Use of Laboratory Animals (National Institutes of Health, USA), and the Guidelines and Policies for Animal Surgery provided by the Animal Study Committees of the Central Institute for Experimental Animals and Keio University.

2.2. Mixed leukocyte reactions (MLR)

The peripheral blood mononuclear cells (PBMCs) in CM were prepared using Lymphoprep (Fresenius Kabi Norge, Halden, Norway). Then, PBMCs were divided into stimulators and responders. The stimulators irradiated at 40 Gy were co-cultured with responders (each 1×10^5 cells) in triplicate in 96 U-well plates (Costar Corp.) for 6 days. PHA (phytohaemagglutinin, Sigma, 2 μg/mL), autologous PBMCs, and allogeneic PBMCs were used as controls in each experiment. The cultures were pulsed with 18.5 kBq/well [^{3}H]-thymidine (Amersham) for 8 h on day 6, and then harvested onto fiber-coated 96-well plates (Packard Instruments, Groningen, Netherlands). Radioactivity was measured using a Top count (Packard Instruments).

2.3. Cell culture and flowcytometric analysis

DCs were generated from bone marrow (BM) cells as previously described (Ohta et al., 2008). Femurs and tibiae of CM were removed and left in 70% ethanol for a few minutes before washing in phosphate buffered saline (PBS). Both ends were cut with scissors and BM cells were cultured in RPMI-1640 supplemented with 10% heat-inactivated fetal calf serum (FCS). After overnight incubation, suspended cells were collected and further cultured in a complete medium (cRPMI), which consisted of RPMI-1640 supplemented with 10% FCS, penicillin and streptomycin (50 U/mL, Invitrogen, Carlsbad, CA), recombinant human (rh) GM-CSF (100 ng/mL; Leukine, Berlex Laboratories, Richmond, CA), and rhIL-4 (100 ng/mL; PeproTech Inc, Rocky Hills, NY). Half the supernatant was replenished with fresh cRPMI on culture day 4, and the floating cells were collected as a DC-enriched cell fraction on culture day 7. On day 7 of culture, cells were stained with anti-human CD11c (clone S-HCL-3, Becton Dickinson, San Jose, CA) and anti-human HLA-DR (clone G46-6, BD Pharmingen, San Diego, CA) antibodies, and then double positive cells were sorted using FACS vantage (BD Biosciences, San Jose, CA) and Moflo (Dako Cytometry, Kyoto, Japan).

2.4. Electron microscopy analysis

Cells were fixed with 2.5% glutaraldehyde and 4% paraformaldehyde (PFA) in 0.1 M cacodylate buffer (pH 7.4) and post-fixed with 1% OsO_4. After dehydration in a graded ethanol series, the cells were embedded in Epon (Oukenshoji, Tokyo). After preparation of semithin sections (0.1 μm), images were obtained using an electron microscope (Japanese Electronic Optical Laboratories, JEOL-1230).

2.5. Magnetic resonance imaging (MRI)

The magnitude of the SCI was monitored by examining changes in intramedullary magnetic resonance imaging (MRI) signals (Metz et al., 2000). MR imaging were performed by using a 7.0 T MR imager (PharmaScan 70/16; Bruker Biospin, Ettlingen, Germany) equipped with the integrated transmitting and receiving coil (i.d. 62 mm) under following conditions: sagittal, coronal, axial T2-weighted fast spin-echo, and sagittal T1-weighted spin-echo.

2.6. Histological analyses

Eight weeks after DC-transplantation, the CM models were perfused with 4% PFA. The dissected spinal cord tissues were post-fixed overnight in 4% PFA, then soaked overnight in 10% followed by 30% sucrose. Serial axial sections (12 μm thickness) were collected every 600 μm over a length of 7200 μm (rostral 1200 μm and caudal 6000 μm to the epicenter). For hematoxylin–eosin (HE) staining, sagittal sections containing the epicenter were also prepared. Some sections were stained with anti-choline acetyltransferase (ChAT) antibody (Ab) (1:200, mouse IgG; Chemicon International, Inc., Temecula, CA), followed by a horseradish peroxidase [HRP]-labeled anti-mouse IgG (1:400, goat IgG; Jackson Laboratory, Bar Harbor, ME). The ABC method was used to detect labeled cells using a Vectastain kit (Vector Laboratories, Burlingame, CA). Sections were also stained with anti-calmodulin-dependent protein kinase IIα (CaMK-IIα) Ab (1:50, mouse monoclonal; Zymed, CA), to detect the corticospinal tract (CST), followed by a secondary antibody, Alexa Fluor 568-conjugated anti-mouse IgG (1:400, goat IgG; Invitrogen).

The myelinated area was analyzed by staining with Luxol fast blue (LFB, Sigma). Images were obtained using Zeiss AxioCam 4.4 (Zeiss) and were converted into binary images using NIH Image software. In the converted binary images, areas with a higher staining intensity than the threshold of LFB staining were defined as myelinated areas. The threshold values were maintained at a constant level for all the analyses. Motor neurons in the ventral horn were analyzed using ChAT staining, and the corticospinal tract area was analyzed using CaMK-IIα staining. Images were

obtained using Zeiss AxioCam 4.4, and these images were analyzed using NIH Image software.

2.7. Behavioral analyses

The behavioral tests were examined according to the previous reports (Iwanami et al., 2005b). They can be summarized as follows.

2.7.1. Bar grip test

The motor function of the upper extremities was evaluated by the bar grip test using device (220 mm wide, 500 mm deep, and 400 mm high with a bar diameter of 2.5 mm in a 1×3 [70 mm $\times$ 100 mm] grid pattern), which analyzes the animal's gripping reflex (the motion undertaken when attempting to grasp an object placed before the animal). The percentage of the maximal grip strength relative to that before the injury was calculated for each day after the injury.

2.7.2. The behavioral scoring test

Each CM was observed for 5 min to assess its ability to perform the basic motions, scored as follows (Iwanami et al., 2005b): score 1, changing from a supine to a prone position; score 2, grasping the cage with its forelimbs; score 3, rasping the cage with its hindlimbs; score 4, walking, with weight bearing, on its forelimbs; score 5, walking, with weight bearing on its hindlimbs; score 6, a single jump; score 7, multiple jumps; score 8, sitting or standing for more than 3 s; and score 9, smooth movements without falling through the gaps between the cage bars. Each animal's score was determined by two independent observers. With scores ranging from 1 to 9, one score was given for each representative motion that was accomplished successfully.

The bargrip test and the behavioral scoring test were performed in a double-blinded manner.

2.7.3. Measurements of spontaneous motor activity

Cages (350 mm wide, 500 mm deep, and 500 mm high) were equipped with infrared sensors (Murata Manufacturing Corp., Nagaokakyo, Kyoto, Japan) on the ceiling to continually record the 3D motion of CMs. This system utilizes a passive thermographic infrared sensor to monitor the heat emitted from the animals. The 3D localization of the heat source was monitored, and a change in this localization was recorded as movement. Each animal's data were recorded and monitored on a computer on an hourly basis, and the activity count after SCI was calculated as a percentage relative to that before the injury.

2.8. Statistical analysis

Student's *t*-test was used to analyze statistically significant differences in immunohistochemical results. The Mann–Whitney *U*-test was used to analyze statistically significant differences in behavioral test results. Data are presented as the mean ± standard error of the mean (SEM) with $^{*}P < 0.05$, $^{**}P < 0.01$, and $^{***}P < 0.001$.

3. Results

3.1. Identification of donor-and-host pairs for DC-transplantation

In this study, DCs were generated from the BM of a CM twin and the generated DCs were transplanted into the other CM twin. To exclude the possibility of allograft rejection between dizygotic twins, an MLR assay was performed. The MLR assay results for the 27 pairs of CM twins are shown in Table 1. Twenty-one of the 27 pairs of CM twins were MLR negative and were used as donor–host pairs for transplantation. In contrast, 6 pairs of the CM twins were

Table 1
Results of the mixed leukocyte reactions (MLR) assay for the screening of donor–host pair.

Twins	PHA	Auto	Allo	Check	Twins	PHA	Auto	Allo	Check	Twins	PHA	Auto	Allo	Check
A1	1606 ± 661	100 ± 11	247 ± 43	99 ± 26	L1	2626 ± 1529	100 ± 7	151 ± 10	127 ± 14	a1	1050 ± 327	100 ± 47	175 ± 54	188 ± 46
A2	1407 ± 1023	100 ± 31	331 ± 52	133 ± 4	L2	6738 ± 966	100 ± 10	149 ± 22	116 ± 18	a2	1848 ± 903	100 ± 36	277 ± 102	122 ± 25
B1	2129 ± 387	100 ± 54	143 ± 45	78 ± 15	M1	446 ± 55	100 ± 9	162 ± 29	96 ± 12	b1	553 ± 101	100 ± 9	110 ± 8	116 ± 9
B2	2194 ± 227	100 ± 14	377 ± 45	84 ± 16	M2	1407 ± 1023	100 ± 31	331 ± 52	133 ± 4	b2	16682 ± 3312	100 ± 39	159 ± 32	131 ± 16
C1	663 ± 385	100 ± 18	814 ± 138	121 ± 6	N1	2935 ± 1709	100 ± 18	109 ± 14	96 ± 15	c1	3813 ± 810	100 ± 22	170 ± 57	394 ± 204
C2	782 ± 112	100 ± 41	143 ± 85	107 ± 14	N2	6464 ± 926	100 ± 12	150 ± 21	121 ± 23	c2	661 ± 278	100 ± 41	202 ± 60	413 ± 109
D1	7898 ± 1625	100 ± 8	197 ± 65	100 ± 16	O1	7607 ± 3201	100 ± 8	673 ± 111	68 ± 4	d1	4505 ± 822	100 ± 21	139 ± 14	123 ± 10
D2	2795 ± 520	100 ± 16	144 ± 14	83 ± 8	O2	9234 ± 3652	100 ± 25	206 ± 12	291 ± 84	d2	60202 ± 1195	100 ± 11	121 ± 13	149 ± 16
E1	7130 ± 1623	100 ± 16	86 ± 14	100 ± 17	P1	4176 ± 1507	100 ± 6	225 ± 14	127 ± 3	e1	7295 ± 2274	100 ± 10	128 ± 3	121 ± 19
E2	18613 ± 232	100 ± 24	280 ± 11	148 ± 63	P2	1373 ± 290	100 ± 19	212 ± 21	103 ± 44	e2	4590 ± 1599	100 ± 11	113 ± 6	122 ± 34
F1	15409 ± 1967	100 ± 12	163 ± 44	113 ± 22	Q1	1848 ± 903	100 ± 36	277 ± 102	122 ± 25	f1	3491 ± 2033	100 ± 19	243 ± 16	224 ± 74
F2	17692 ± 2033	100 ± 13	190 ± 35	104 ± 17	Q2	4785 ± 437	100 ± 14	347 ± 134	90 ± 11	f2	3740 ± 536	100 ± 20	168 ± 33	260 ± 118
G1	4651 ± 1399	100 ± 31	470 ± 305	125 ± 30	R1	30370 ± 6250	100 ± 17	179 ± 19	100 ± 8					
G2	678 ± 43	100 ± 10	158 ± 37	90 ± 43	R2	17962 ± 3345	100 ± 8	131 ± 20	119 ± 19					
H1	5219 ± 805	100 ± 10	635 ± 71	141 ± 6	S1	42365 ± 9643	100 ± 7	156 ± 9	111 ± 19					
H2	1380 ± 810	100 ± 24	200 ± 39	162 ± 28	S2	6555 ± 1606	100 ± 40	151 ± 12	108 ± 29					
I1	953 ± 207	100 ± 28	145 ± 6	90 ± 24	T1	2742 ± 487	100 ± 15	161 ± 24	131 ± 14					
I2	8735 ± 810	100 ± 32	444 ± 207	107 ± 26	T2	41893 ± 8601	100 ± 14	152 ± 14	106 ± 14					
J1	398 ± 70	100 ± 45	301 ± 174	145 ± 27	U1	14329 ± 2610	100 ± 24	159 ± 37	140 ± 30					
J2	1537 ± 399	100 ± 13	127 ± 66	129 ± 54	U2	1220 ± 727	100 ± 13	145 ± 13	83 ± 15					
K1	2710 ± 52	100 ± 12	296 ± 38	100 ± 18										
K2	760 ± 75	100 ± 16	224 ± 31	105 ± 10										

The value of autologous reaction is referred to 100. Each value indicates the percentage of radioactivity relative to that of autologous reaction (mean ± SD). Twenty-one pairs of twins (A–U) are MLR negative and 6 pairs of twins (a–f) are MLR positive.

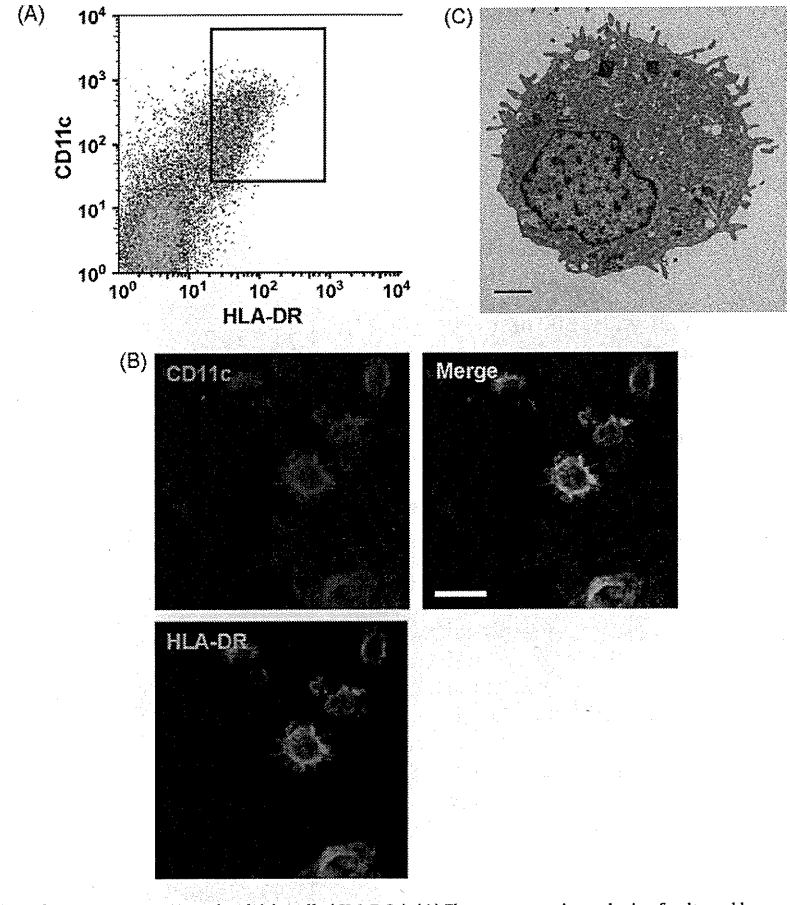

Fig. 1. Purification and characterization of common marmoset dendritic cells (CM-DCs). (A) Flow cytometric analysis of cultured bone marrow (BM) in the presence of rhGM-CSF and rhIL-4 for a week. $CD11c^{+}HLA\text{-}DR^{+}$ cells (boxed area) were isolated as CM-DCs. (B) Typical images of CM-DCs stained for CD11c (red) and HLA-DR (green) antibodies. Scale bar, 20 μm. (C) Electron microscopic analysis of CM-DCs. Scale bar, 1 μm. (For interpretation of the references to color in this figure legend, the reader is referred to the web version of the article.)

MLR positive and thus were not used for further DC-transplantation experiments.

3.2. Purification and characterization of DCs from bone marrow

DCs were cultured for a week in the presence of hrGM-CSF and hrIL-4 from the BM of CM as described previously (Ohta et al., 2008). CM-DCs were purified as cells double-labeled for CD11c and HLA-DR antibodies using flow cytometry (Fig. 1A). Approximately 4–8 × 10^6 DCs were purified from 1 to 5 × 10^8 BM cells of a CM. A typical image of BM-derived DCs stained with CD11c and HLA-DR antibodies is shown in Fig. 1B. Electron microscopic analysis of CM-DCs showed an eccentric nucleus and the presence of small dendrites consistent with typical DC morphology (Fig. 1C).

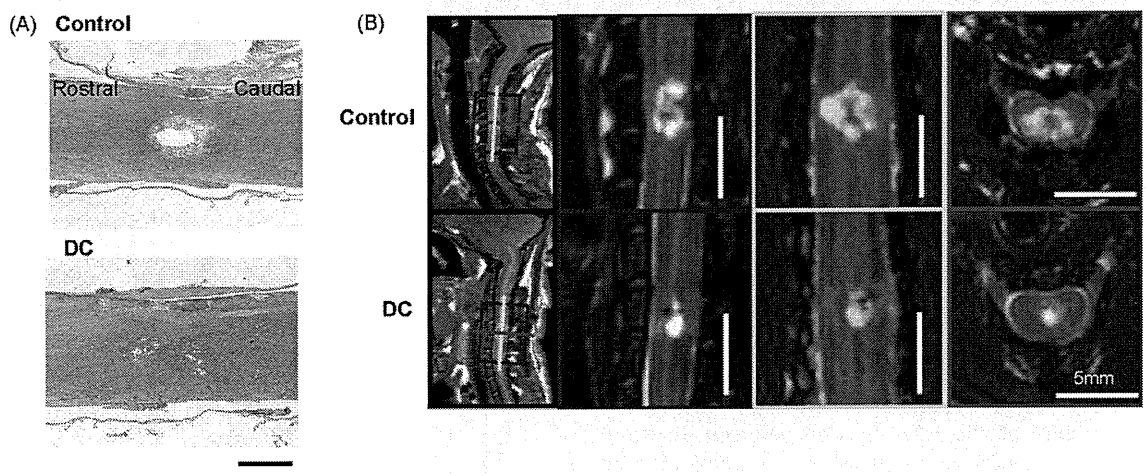

Fig. 2. Histological and magnetic resonance images (MRI) of the injured spinal cord in CMs 8 weeks after DC-transplantation. (A) H&E staining of sagittal sections of injured spinal cords in DC-transplanted CM (animal No. U2 in Table 1) and control. Scale bar, 1 mm. (B) Sagittal, coronal, and axial MR images (T2WI) of injured spinal cords in CMs. The DC-treated CM is animal No. B1. The lesion was visible as a hyperintense signal on T2WI-MRI. Scale bar, 5 mm.

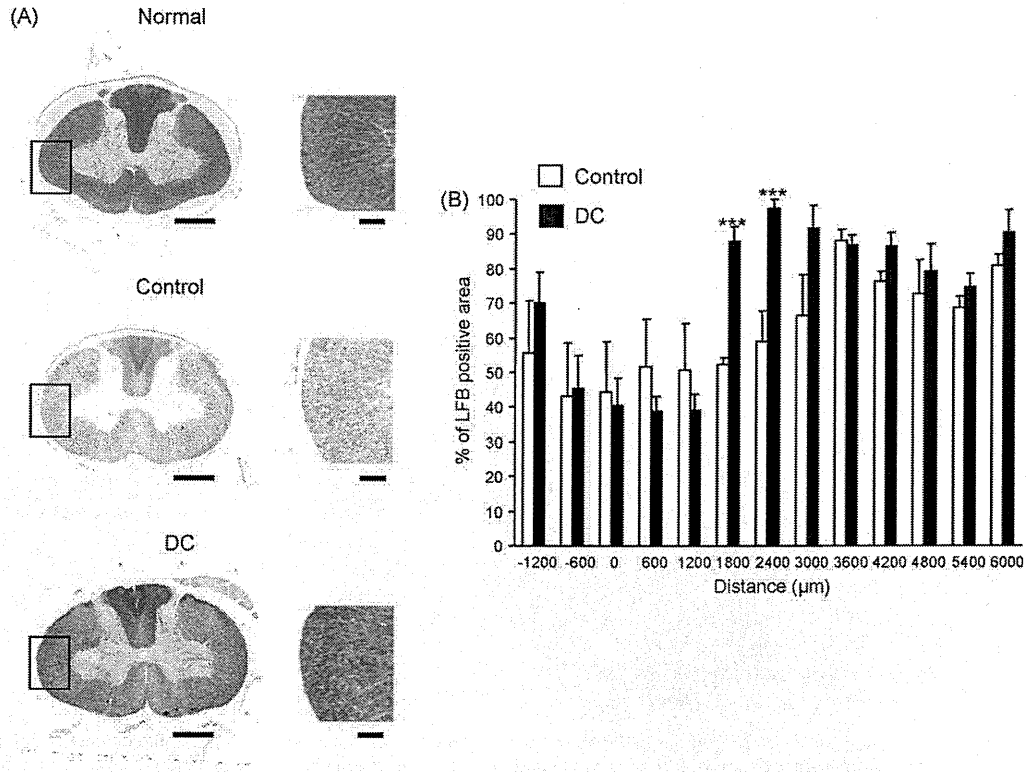

Fig. 3. Quantitative analysis of myelinated areas around the epicenter 8 weeks after transplantation. (A) Representative LFB-stained specimens from normal CM, control CM and DC-treated CM (animal No. O1). Scale bar, 1 mm. Scale bar for enlarged image of boxed area, 250 μm. (B) Cranio-caudal distribution (total length of 7200 μm; 1200 μm rostral (−) and 6000 μm caudal (+) to the epicenter) of the LFB-positive area in control and DC-treated CMs. The percentage of the LFB-positive area relative to the corresponding area in the intact CM was calculated using NIH image software. DCs-treatment, $n = 6$; control, $n = 5$. ***$P < 0.001$.

3.3. Lesion size reduction with DC-transplantation

Seven days after injury, 4–8 × 10^6 DCs generated from the BM of a donor CM twin were transplanted into the injured site of the spinal cord of a host CM twin. Histochemical analysis showed the spinal cord lesion to be smaller in a DC-transplanted CM than in a control 8 weeks after DC-transplantation (Fig. 2A). On MRI, T2-weighted images (T2WI) showed a hyperintense signal in the injured spinal cord of the control CM 8 weeks after injury and the signal in the DC-transplanted CM was smaller than that of control (Fig. 2B).

3.4. Immunohistochemical analyses

Axial sections of spinal cords in either DC- or RPMI-treated CMs 8 weeks after transplantation were subjected to immunological analyses to determine the effects of DC-transplantation. We collected serial axial sections every 12 μm in a total length of 7200 μm (1200 μm rostral and 6000 μm caudal to the epicenter). The LFB staining showed a decrease in demyelinated areas caudal to the epicenter in DC-transplanted CMs as compared to that of controls (Fig. 3). In a monkey, CST fibers project to the ventral horn, and some axons synapse directly on motor neurons innervating hand muscles (Lemon et al., 2004). The number of ChAT-positive motor neurons in the ventral horn was greater in DC-treated CMs than in controls in areas caudal to the lesion site (Fig. 4). We further measured the density of nerve fibers that stained positively for CaMK-IIα (Terashima et al., 1994). CaMK-IIα-positive CST fibers were observed in the lateral funiculus, and immunoreactivity of CaMK-IIα in DC-treated CMs was greater than that in controls in some areas caudal to the lesion site (Fig. 5).

3.5. Behavioral recovery after DC-transplantation

To examine the effect of DC-transplantation, we performed three different behavioral analyses established by Iwanami et al. (2005a); bar grip test, behavior scoring tests, and measurement of spontaneous motor activity. The corticospinal system is involved in dexterous hand movements. To evaluate the recovery of forelimb motor function, bar grip tests were conducted on described days. The bar grip strength sharply decreased in both groups immediately after injury. After transplantation, DC-treated CMs showed significant recovery, with higher bar grip power values than the controls at 1, 3, 7, and 8 weeks after transplantation (Fig. 6A). The behavioral scoring test assesses the recovery of motor function in the forelimbs and hindlimbs (Iwanami et al., 2005b). DC-treated groups showed significant recovery as compared to controls at 1, 4, and 5 weeks after transplantation (Fig. 6B). In the measurement of spontaneous three-dimensional movement using a sensor placed in the cages, the values in both groups decreased sharply after injury. After DC-transplantation, DC-treated animals tended to show earlier recovery than controls, although the difference was not statistically significant (Fig. 6C).

The monitoring of spontaneous 3D movement is an objective behavior analysis; however, such monitoring assesses not only motor function, but also general physical condition. Thus, the general physical condition of the mice might have affected the results. Further behavior analyses will be required to assess the details of motor function in CMs after SCI.

4. Discussion

Our current results demonstrate that transplantation of DCs contributes to the functional recovery of SCI in a non-human

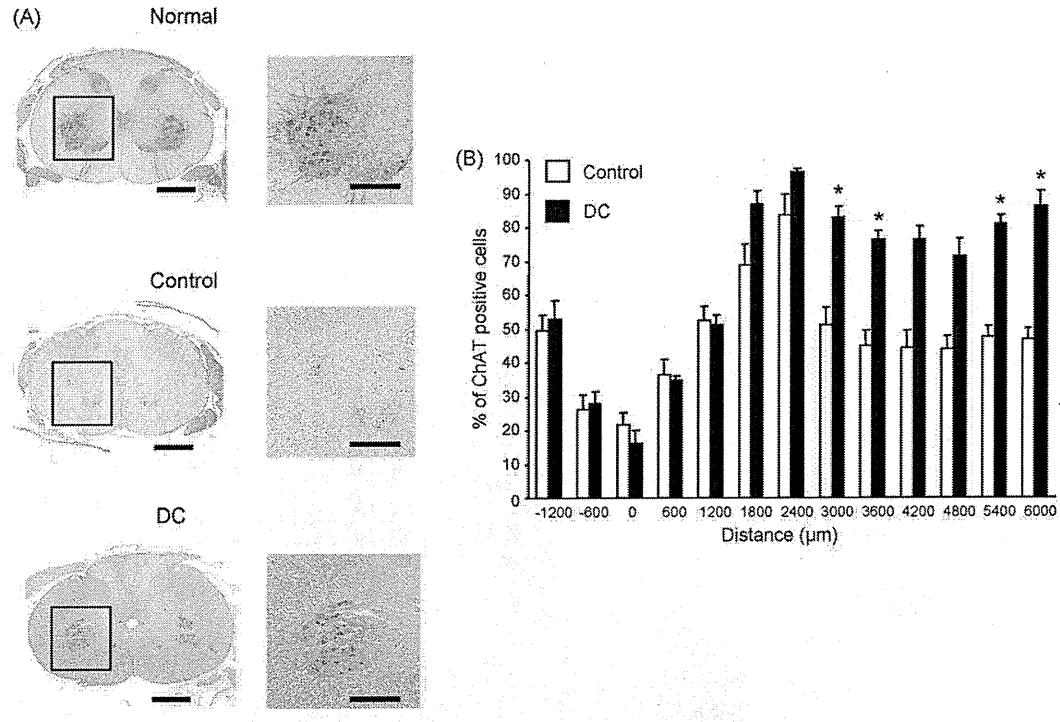

Fig. 4. Quantitative analysis of the number of ChAT-positive neurons in the ventral horn around the epicenter 8 weeks after transplantation. (A) Anti-ChAT immunostaining. ChAT-positive cells are observed in the ventral horn of the spinal cord as shown in the boxed area. The DC-treated CM is animal No. O1. Scale bar, 1 mm. Scale bar for enlarged image of boxed area, 500 μm. (B) Cranio-caudal distribution (total length of 7200 μm; 1200 μm rostral (−) and 6000 μm caudal (+) to the epicenter) of the ChAT-positive area in control and DCs-treated CMs. DC-treatment, $n = 6$; control, $n = 5$. $^*P < 0.05$.

primate SCI model using CM. In our previous study using a mouse SCI model, DC-transplantation enhanced axonal sprouting caudal to the lesion site (Mikami et al., 2004). One of the mechanisms underlying the enhancement of axonal sprouting by DCs is suggested to be increased NT-3 level, within the injured spinal cord, which is secreted from implanted mouse DCs. NT-3 is known to promote axonal growth in the spinal cord (Grill et al., 1997) and support the remyelination in SCI (McTigue et al., 1998; Girard et al., 2005). Recently, we demonstrated that CM-DCs also express NT-3 (Ohta et al., 2008). In this study, immunohistochemical analyses showed a decrease in neuronal loss and demyelination in the areas caudal to the lesion site in response to DC-transplantation. Although further studies are required to analyze descending fibers including CST in the CM-SCI model in detail, NT-3 secreted by DCs may exert a neuroprotective effect by decreasing neuronal loss and axonal damage.

We previously demonstrated the *de-novo* neurogenesis accompanied by the increase in NSPCs after DC-transplantation in a mouse SCI model (Mikami et al., 2004). In this study, we could not analyze either neurogenesis or NSPCs in the injured CM spinal cord due to technical difficulties. However, in our preliminary study, CM-DCs increased the number of human NSPCs *in vitro* (unpublished data). Thus, CM-DCs might have increased the number of neurons in the spinal cord via *de-novo* neurogenesis accompanied by the activation of endogenous NSPCs. It is also possible that activation of endogenous NSPCs might increase oligodendrocyte

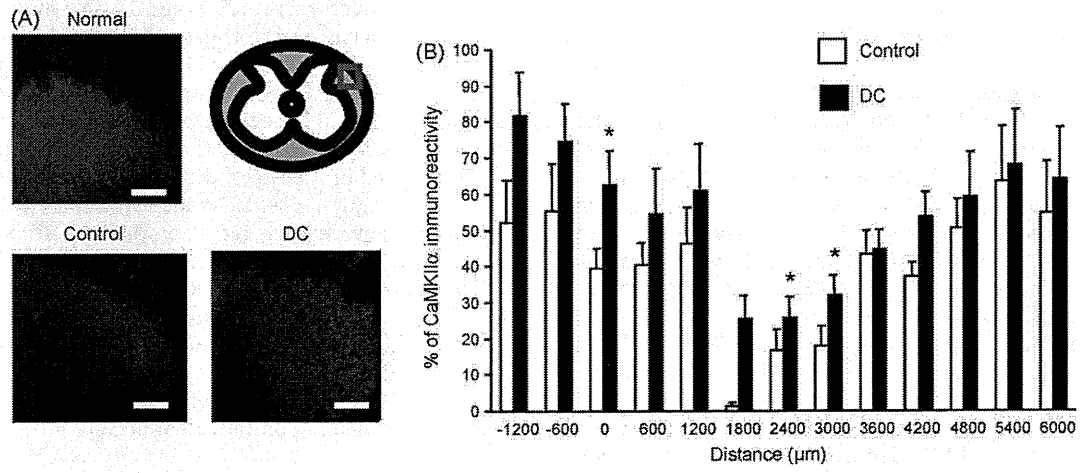

Fig. 5. Quantitative analysis of CaMK-IIα positive area around the epicenter 8 weeks after transplantation. (A) Enlarged images of boxed areas that are stained with CaMK-IIα antibody in the lateral funiculus are shown. The DC-treated CM is animal No. O1. Scale bar, 100 μm. (B) Cranio-caudal distribution (total length of 7200 μm; 1200 μm rostral (−) and 6000 μm caudal (+) to the epicenter) of the CaMK-IIα positive area (boxed area in A) in control and DC-treated CMs. The percentage of the CaMK-IIα positive area relative to the corresponding area in the intact CM was calculated using NIH image software. DCs-treatment, $n = 6$; control, $n = 5$. $^*P < 0.05$.

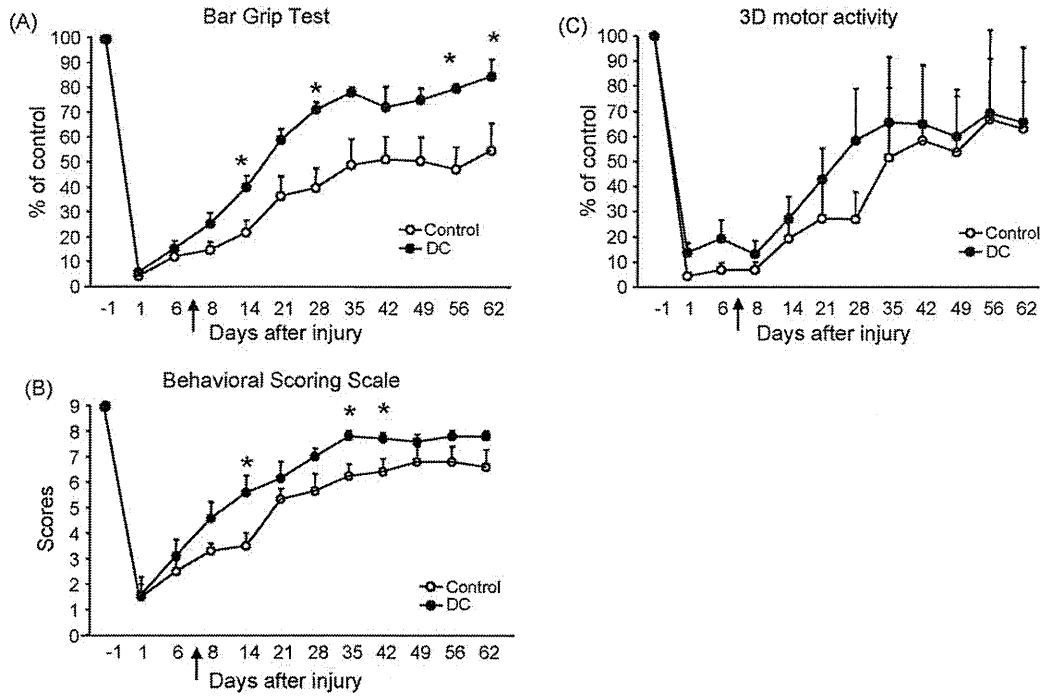

Fig. 6. Behavioral analyses of SCI-CMs after DC-transplantation. (A) Bar grip test. The time course of the bar grip power in control and DCs-treated CMs. Each value indicates the percentage of bar grip power before injury (DC-treatment, $n = 5$; control, $n = 5$). (B) Behavioral scoring scale. The scores (1–9 points) was given for each representative motion, as described in Section 2 (DC-treatment, $n = 5$; control, $n = 5$). (C) 3D measurements of spontaneous motor activity. The value indicates the percentage of spontaneous motor activity before injury (DC-treatment, $n = 5$; control, $n = 5$). Arrow indicates the day of DC-treatment. $^*P < 0.05$, Mann–Whitney U-test.

progenitors, leading to the enhancement of remyelination. Future studies are required to analyze endogenous NSPCs in CM *in vivo*.

Several reports of immune-cell-based therapy have described the treatment of SCI. Activated microglia have been shown to secrete neurotrophins *in vitro* (Elkabes et al., 1996; Miwa et al., 1997; Nakajima et al., 2001) and *in vivo* (Batchelor et al., 1999; Bouhy et al., 2006). These neurotrophins promote neuronal survival and axonal regeneration in SCI (Prewitt et al., 1997; Rabchevsky and Streit, 1997). Recently, skin-derived macrophages (Knoller et al., 2005) and bone marrow cells with GM-CSF (Yoon et al., 2007) showed beneficial effects on SCI in clinical studies. One of advantages of DC therapy is that autologous transplantation can be performed; DCs are generated from monocytes in peripheral blood of patients within a week (Babatz et al., 2003). The therapeutic time window including the timing of such treatment is important in SCI therapy. Many studies suggest that delayed administration (1–2 weeks after SCI) of cells is suitable for the treatment of SCI (Ogawa et al., 2002; Okano, 2002; Okada et al., 2005; Bouhy et al., 2006; Iarikov et al., 2007; Iwanami et al., 2005a), because inflammatory reactions in the acute phase may inhibit survival of transplanted cells. Considering how easily such cells can be obtained, the timing of the treatment, and the lack of allograft problems, DC are a useful cell type for SCI therapy in humans.

In this study $4–8 \times 10^6$ DCs generated from BM cells were transplanted into the spinal cord, although the same number of DCs should be transplanted in each animal. In our previous study, one million cells were implanted into the mouse spinal cord (Mikami et al., 2004). If the same cell number per body weight is used, approximately 10 million cells should be transplanted into each CM. However, it is very difficult to obtain 10 million cells from a donor CM. In clinical studies, various cell numbers of immune cells (4–200 million cells) were transplanted into the human spinal cord (Knoller et al., 2005; Yoon et al., 2007). From human peripheral blood, 100 million DCs can be obtained (Motta et al., 2003). Therefore, we transplanted the maximum cell number of DCs obtained from a donor CM in each experiment. In addition, in the protocol of this study, we performed DC sorting and the surgery for the DC-transplantation on the same day. The number of DCs generated *in vitro* from the same number of BM cells differed among the experiments, since the yield of DCs depended upon individual factors (Ohta et al., 2008). A considerable length of time was required to sort the DCs using FACS because of the small population of CM-DCs in the BM cultures. These technical problems also caused the cell number of DCs used for transplantation to differ among the experiments. In future studies progressing toward clinical application, the cell number of DCs used for transplantation into the spinal cord will need to be optimized.

The safety of DCs for cancer therapy has already been demonstrated in humans. Observations of the general health conditions revealed no apparent differences between control and DC-treated CMs. In this study, we also followed weight changes to monitor health conditions during the experiments. No significant weight loss was observed in CMs after DC-transplantation. Moreover, the spontaneous movements of the DC-treated CMs were always better than those of the control CMs, although the difference was not statistically significant (Fig. 6C). In the histological analyses, no apparent additional damage to the spinal cord was observed after DC-transplantation. Although further safety studies are required to realize clinical applications, these results suggest the safety of administering DCs into spinal cord lesions.

Compared with rodents, CMs have distinct differences in anatomy and functional neural circuits of the spinal cord (Fujiyoshi et al., 2007). Thus, our study in CMs may be important for the preclinical evaluation of DC therapy for human SCI. DC-transplantation showed a neuroprotective effect on SCI, leading to functional recovery in CMs. Taken together, our results suggest that DC therapy has major potential for the treatment of SCI in the clinical setting.

Acknowledgments

This work was supported by grants from the Ministry of Education, Culture, Sports, Science and Technology (MEXT), Japan and a Grant-in-aid for the Global COE program to Keio University from MEXT. We thank Dr. F. Toyota, Dr. H. Ishi, and Y. Tanioka (Central Institute for Experimental Animals) for their technical assistant with the operations and the animal care of CMs. We thank M. Kokubo, T. Muraki, and S. Teramoto (Keio University School of Medicine) for technical assistance.

References

Abbott, D.H., Barnett, D.K., Colman, R.J., Yamamoto, M.E., Schultz-Darken, N.J., 2003. Aspects of common marmoset basic biology and life history important for biomedical research. Comp. Med. 53 (4), 339–350.

Babatz, J., Rollig, C., Oelschlagel, U., Zhao, S., Ehninger, G., Schmitz, M., Bornhauser, M., 2003. Large-scale immunomagnetic selection of CD14+ monocytes to generate dendritic cells for cancer immunotherapy: a phase I study. J. Hematother. Stem Cell Res. 12 (5), 515–523.

Banchereau, J., Palucka, A.K., 2005. Dendritic cells as therapeutic vaccines against cancer. Nat. Rev. Immunol. 5 (4), 296–306.

Barros, M., Boere, V., Huston, J.P., Tomaz, C., 2000. Measuring fear and anxiety in the marmoset (*Callithrix penicillata*) with a novel predator confrontation model: effects of diazepam. Behav. Brain Res. 108 (2), 205–211.

Batchelor, P.E., Liberatore, G.T., Wong, J.Y., Porritt, M.J., Frerichs, F., Donnan, G.A., Howells, D.W., 1999. Activated macrophages and microglia induce dopaminergic sprouting in the injured striatum and express brain-derived neurotrophic factor and glial cell line-derived neurotrophic factor. J. Neurosci. 19 (5), 1708–1716.

Bouhy, D., Malgrange, B., Multon, S., Poirrier, A.L., Scholtes, F., Schoenen, J., Franzen, R., 2006. Delayed GM-CSF treatment stimulates axonal regeneration and functional recovery in paraplegic rats via an increased BDNF expression by endogenous macrophages. FASEB J. 20 (8), 1239–1241.

Courtine, G., Bunge, M.B., Fawcett, J.W., Grossman, R.G., Kaas, J.H., Lemon, R., Maier, I., Martin, J., Nudo, R.J., Ramon-Cueto, A., Rouiller, E.M., Schnell, L., Wannier, T., Schwab, M.E., Edgerton, V.R., 2007. Can experiments in nonhuman primates expedite the translation of treatments for spinal cord injury in humans? Nat. Med. 13 (5), 561–566.

Cummings, B.J., Uchida, N., Tamaki, S.J., Salazar, D.L., Hooshmand, M., Summers, R., Gage, F.H., Anderson, A.J., 2005. Human neural stem cells differentiate and promote locomotor recovery in spinal cord-injured mice. Proc. Natl. Acad. Sci. U.S.A. 102 (39), 14069–14074.

Doucette, R., 1995. Olfactory ensheathing cells: potential for glial cell transplantation into areas of CNS injury. Histol. Histopathol. 10 (2), 503–507.

Elkabes, S., DiCicco-Bloom, E.M., Black, I.B., 1996. Brain microglia/macrophages express neurotrophins that selectively regulate microglial proliferation and function. J. Neurosci. 16 (8), 2508–2521.

Fouad, K., Klusman, I., Schwab, M.E., 2004. Regenerating corticospinal fibers in the Marmoset (*Callitrix jacchus*) after spinal cord lesion and treatment with the anti-Nogo-A antibody IN-1. Eur. J. Neurosci. 20 (9), 2479–2482.

Fujiyoshi, K., Yamada, M., Nakamura, M., Yamane, J., Katoh, H., Kitamura, K., Kawai, K., Okada, S., Momoshima, S., Toyama, Y., Okano, H., 2007. In vivo tracing of neural tracts in the intact and injured spinal cord of marmosets by diffusion tensor tractography. J. Neurosci. 27 (44), 11991–11998.

Girard, C., Bemelmans, A.P., Dufour, N., Mallet, J., Bachelin, C., Nait-Oumesmar, B., Baron-Van Evercooren, A., Lachapelle, F., 2005. Grafts of brain-derived neurotrophic factor and neurotrophin 3-transduced primate Schwann cells lead to functional recovery of the demyelinated mouse spinal cord. J. Neurosci. 25 (35), 7924–7933.

Gnanalingham, K.K., Smith, L.A., Hunter, A.J., Jenner, P., Marsden, C.D., 1993. Alterations in striatal and extrastriatal D-1 and D-2 dopamine receptors in the MPTP-treated common marmoset: an autoradiographic study. Synapse 14 (2), 184–194.

Grill, R., Murai, K., Blesch, A., Cage, F.H., Tuszynski, M.H., 1997. Cellular delivery of neurotrophin-3 promotes corticospinal axonal growth and partial functional recovery after spinal cord injury. J. Neurosci. 17 (4), 5560–5572.

Hauben, E., Nevo, U., Yoles, E., Moalem, G., Agranov, E., Mor, F., Akselrod, S., Neeman, M., Cohen, I.R., Schwartz, M., 2000. Autoimmune T cells as potential neuroprotective therapy for spinal cord injury. Lancet 355 (9200), 286–287.

Iarikov, D.E., Kim, B.G., Dai, H.N., McAtee, M., Kuhn, P.L., Bregman, B.S., 2007. Delayed transplantation with exogenous neurotrophin administration enhances plasticity of corticofugal projections after spinal cord injury. J. Neurotrauma 24 (4), 690–702.

Iwanami, A., Kaneko, S., Nakamura, M., Kanemura, Y., Mori, H., Kobayashi, S., Yamasaki, M., Momoshima, S., Ishii, H., Ando, K., Tanioka, Y., Tamaoki, N., Nomura, T., Toyama, Y., Okano, H., 2005a. Transplantation of human neural stem cells for spinal cord injury in primates. J. Neurosci. Res. 80 (2), 182–190.

Iwanami, A., Yamane, J., Katoh, H., Nakamura, M., Momoshima, S., Ishii, H., Tanioka, Y., Tamaoki, N., Nomura, T., Toyama, Y., Okano, H., 2005b. Establishment of graded spinal cord injury model in a nonhuman primate: the common marmoset. J. Neurosci. Res. 80 (2), 172–181.

Kendall, A.L., Rayment, F.D., Torres, E.M., Baker, H.F., Ridley, R.M., Dunnett, S.B., 1998. Functional integration of striatal allografts in a primate model of Huntington's disease. Nat. Med. 4 (6), 727–729.

Knoller, N., Auerbach, G., Fulga, V., Zelig, G., Attias, J., Bakimer, R., Marder, J.B., Yoles, E., Belkin, M., Schwartz, M., Hadani, M., 2005. Clinical experience using incubated autologous macrophages as a treatment for complete spinal cord injury: phase I study results. J. Neurosurg. Spine 3 (3), 173–181.

Koda, M., Okada, S., Nakayama, T., Koshizuka, S., Kamada, T., Nishio, Y., Someya, Y., Yoshinaga, K., Okawa, A., Moriya, H., Yamazaki, M., 2005. Hematopoietic stem cell and marrow stromal cell for spinal cord injury in mice. Neuroreport 16 (16), 1763–1767.

Koshizuka, S., Okada, S., Okawa, A., Koda, M., Murasawa, M., Hashimoto, M., Kamada, T., Yoshinaga, K., Murakami, M., Moriya, H., Yamazaki, M., 2004. Transplanted hematopoietic stem cells from bone marrow differentiate into neural lineage cells and promote functional recovery after spinal cord injury in mice. J. Neuropathol. Exp. Neurol. 63 (1), 64–72.

Lemon, R.N., Kirkwood, P.A., Maier, M.A., Nakajima, K., Nathan, P., 2004. Direct and indirect pathways for corticospinal control of upper limb motoneurons in the primate. Prog. Brain Res. 143, 263–279.

Liu, S., Aghakhani, N., Boisset, N., Said, G., Tadie, M., 2001. Innervation of the caudal denervated ventral roots and their target muscles by the rostral spinal motoneurons after implanting a nerve autograft in spinal cord-injured adult marmosets. J. Neurosurg. 94 (1 Suppl.), 82–90.

Ludlage, E., Mansfield, K., 2003. Clinical care and diseases of the common marmoset (*Callithrix jacchus*). Comp. Med. 53 (4), 369–382.

Mansfield, K., 2003. Marmoset models commonly used in biomedical research. Comp. Med. 53 (4), 383–392.

Marshall, J.W., Cross, A.J., Jackson, D.M., Green, A.R., Baker, H.F., Ridley, R.M., 2000. Clomethiazole protects against hemineglect in a primate model of stroke. Brain Res. Bull. 52 (1), 21–29.

Martin, D., Robe, P., Franzen, R., Delree, P., Schoenen, J., Stevenaert, A., Moonen, G., 1996. Effects of Schwann cell transplantation in a contusion model of rat spinal cord injury. J. Neurosci. Res. 45 (5), 588–597.

McDonald, J.W., Liu, X.Z., Qu, Y., Liu, S., Mickey, S.K., Turetsky, D., Gottlieb, D.I., Choi, D.W., 1999. Transplanted embryonic stem cells survive, differentiate and promote recovery in injured rat spinal cord. Nat. Med. 5 (12), 1410–1412.

McTigue, D.M., Horner, P.J., Stokes, B.T., Gage, F.H., 1998. Neurotrophin-3 and brain-derived neurotrophic factor induce oligodendrocyte proliferation and myelination of regenerating axons in the contused adult rat spinal cord. J. Neurosci. 18, 5354–5365.

Metz, G.A., Curt, A., van de Meent, H., Klusman, I., Schwab, M.E., Dietz, V., 2000. Validation of the weight-drop contusion model in rats: a comparative study of human spinal cord injury. J. Neurotrauma 17 (1), 1–17.

Mikami, Y., Okano, H., Sakaguchi, M., Nakamura, M., Shimazaki, T., Okano, H.J., Kawakami, Y., Toyama, Y., Toda, M., 2004. Implantation of dendritic cells in injured adult spinal cord results in activation of endogenous neural stem/progenitor cells leading to de novo neurogenesis and functional recovery. J. Neurosci. Res. 76 (4), 453–465.

Miwa, T., Furukawa, S., Nakajima, K., Furukawa, Y., Kohsaka, S., 1997. Lipopolysaccharide enhances synthesis of brain-derived neurotrophic factor in cultured rat microglia. J. Neurosci. Res. 50 (6), 1023–1029.

Motta, M.R., Castellani, S., Rizzi, S., Curti, A., Gubinelli, F., Fogli, M., Ferri, E., Cellini, C., Baccarani, M., Lemoli, R.M., 2003. Generation of dendritic cells from CD14+ monocytes positively selected by immunomagnetic adsorption for multiple myeloma patients enrolled in a clinical trial of anti-idiotype vaccination. Br. J. Haematol. 121 (2), 240–250.

Nakajima, K., Honda, S., Tohyama, Y., Imai, Y., Kohsaka, S., Kurihara, T., 2001. Neurotrophin secretion from cultured microglia. J. Neurosci. Res. 65 (4), 322–331.

Nencioni, A., Brossart, P., 2004. Cellular immunotherapy with dendritic cells in cancer: current status. Stem Cells 22 (4), 501–513.

Ogawa, Y., Sawamoto, K., Miyata, T., Miyao, S., Watanabe, M., Nakamura, M., Bregman, B.S., Koike, M., Uchiyama, Y., Toyama, Y., Okano, H., 2002. Transplantation of in vitro-expanded fetal neural progenitor cells results in neurogenesis and functional recovery after spinal cord contusion injury in adult rats. J. Neurosci. Res. 69 (6), 925–933.

Ohta, S., Ueda, Y., Yaguchi, M., Matsuzaki, Y., Nakamura, M., Toyama, Y., Tanioka, Y., Tamaoki, N., Nomura, T., Okano, H., Kawakami, Y., Toda, M., 2008. Isolation and characterization of dendritic cells from common marmosets for preclinical cell therapy studies. Immunology 123 (4), 566–574.

Okada, S., Ishii, K., Yamane, J., Iwanami, A., Ikegami, T., Katoh, H., Iwamoto, Y., Nakamura, M., Miyoshi, H., Okano, H.J., Contag, C.H., Toyama, Y., Okano, H., 2005. In vivo imaging of engrafted neural stem cells: its application in evaluating the optimal timing of transplantation for spinal cord injury. FASEB J. 19 (13), 1839–1841.

Okano, H., 2002. Stem cell biology of the central nervous system. J. Neurosci. Res. 69 (6), 698–707.

Prewitt, C.M., Niesman, I.R., Kane, C.J., Houle, J.D., 1997. Activated macrophage/microglial cells can promote the regeneration of sensory axons into the injured spinal cord. Exp. Neurol. 148 (2), 433–443.

Rabchevsky, A.G., Streit, W.J., 1997. Grafting of cultured microglial cells into the lesioned spinal cord of adult rats enhances neurite outgrowth. J. Neurosci. Res. 47 (1), 34–48.

Richter, M.W., Roskams, A.J., 2008. Olfactory ensheathing cell transplantation following spinal cord injury: hype or hope? Exp. Neurol. 209 (2), 353–367.

Schuler, G., Schuler-Thurner, B., Steinman, R.M., 2003. The use of dendritic cells in cancer immunotherapy. Curr. Opin. Immunol. 15 (2), 138–147.

Steinman, R.M., 1991. The dendritic cell system and its role in immunogenicity. Annu. Rev. Immunol. 9, 271–296.
Steinman, R.M., Hawiger, D., Nussenzweig, M.C., 2003. Tolerogenic dendritic cells. Annu. Rev. Immunol. 21, 685–711.
t Hart, B.A., Bauer, J., Muller, H.J., Melchers, B., Nicolay, K., Brok, H., Bontrop, R.E., Lassmann, H., Massacesi, L., 1998. Histopathological characterization of magnetic resonance imaging-detectable brain white matter lesions in a primate model of multiple sclerosis: a correlative study in the experimental autoimmune encephalomyelitis model in common marmosets (*Callithrix jacchus*). Am. J. Pathol. 153 (2), 649–663.
t Hart, B.A., Laman, J.D., Bauer, J., Blezer, E., van Kooyk, Y., Hintzen, R.Q., 2004. Modelling of multiple sclerosis: lessons learned in a non-human primate. Lancet Neurol. 3 (10), 588–597.
Takami, T., Oudega, M., Bates, M.L., Wood, P.M., Kleitman, N., Bunge, M.B., 2002. Schwann cell but not olfactory ensheathing glia transplants improve hindlimb locomotor performance in the moderately contused adult rat thoracic spinal cord. J. Neurosci. 22 (15), 6670–6681.
Terashima, T., Ochiishi, T., Yamauchi, T., 1994. Immunohistochemical detection of calcium/calmodulin-dependent protein kinase II in the spinal cord of the rat and monkey with special reference to the corticospinal tract. J. Comp. Neurol. 340 (4), 469–479.
Yoon, S.H., Shim, Y.S., Park, Y.H., Chung, J.K., Nam, J.H., Kim, M.O., Park, H.C., Park, S.R., Min, B.H., Kim, E.Y., Choi, B.H., Park, H., Ha, Y., 2007. Complete spinal cord injury treatment using autologous bone marrow cell transplantation and bone marrow stimulation with granulocyte macrophage-colony stimulating factor (GM-CSF): phase i/ii clinical trial. Stem Cells 25 (8), 2066–2073.

OPEN ACCESS Freely available online

PLoS one

Roles of ES Cell-Derived Gliogenic Neural Stem/Progenitor Cells in Functional Recovery after Spinal Cord Injury

Gentaro Kumagai[1,2,3], Yohei Okada[1,4,5], Junichi Yamane[2], Narihito Nagoshi[1,2], Kazuya Kitamura[1,2], Masahiko Mukaino[1,6], Osahiko Tsuji[1,2], Kanehiro Fujiyoshi[1,2], Hiroyuki Katoh[2], Seiji Okada[7], Shinsuke Shibata[1], Yumi Matsuzaki[1], Satoshi Toh[3], Yoshiaki Toyama[2], Masaya Nakamura[2]*, Hideyuki Okano[1]*

1 Department of Physiology, Keio University School of Medicine, Tokyo, Japan, **2** Department of Orthopedic Surgery, Keio University School of Medicine, Tokyo, Japan, **3** Department of Orthopedic Surgery, Hirosaki University Graduate School of Medicine, Hirosaki, Japan, **4** Department of Neurology, Graduate School of Medicine, Nagoya University, Nagoya, Japan, **5** Kanrinmaru Project, Keio University School of Medicine, Tokyo, Japan, **6** Department of Rehabilitation Medicine, Keio University School of Medicine, Tokyo, Japan, **7** Department of Research Super Star Program Stem Cell Unit, Graduate School of Medical Science, Kyusyu University, Fukuoka, Japan

Abstract

Transplantation of neural stem/progenitor cells (NS/PCs) following the sub-acute phase of spinal cord injury (SCI) has been shown to promote functional recovery in rodent models. However, the types of cells most effective for treating SCI have not been clarified. Taking advantage of our recently established neurosphere-based culture system of ES cell-derived NS/PCs, in which primary neurospheres (PNS) and passaged secondary neurospheres (SNS) exhibit neurogenic and gliogenic potentials, respectively, here we examined the distinct effects of transplanting neurogenic and gliogenic NS/PCs on the functional recovery of a mouse model of SCI. ES cell-derived PNS and SNS transplanted 9 days after contusive injury at the Th10 level exhibited neurogenic and gliogenic differentiation tendencies, respectively, similar to those seen *in vitro*. Interestingly, transplantation of the gliogenic SNS, but not the neurogenic PNS, promoted axonal growth, remyelination, and angiogenesis, and resulted in significant locomotor functional recovery after SCI. These findings suggest that gliogenic NS/PCs are effective for promoting the recovery from SCI, and provide essential insight into the mechanisms through which cellular transplantation leads to functional improvement after SCI.

Citation: Kumagai G, Okada Y, Yamane J, Nagoshi N, Kitamura K, et al. (2009) Roles of ES Cell-Derived Gliogenic Neural Stem/Progenitor Cells in Functional Recovery after Spinal Cord Injury. PLoS ONE 4(11): e7706. doi:10.1371/journal.pone.0007706

Editor: Kenji Hashimoto, Chiba University Center for Forensic Mental Health, Japan

Received August 18, 2009; **Accepted** October 9, 2009; **Published** November 6, 2009

Funding: This work was supported by grants from the Leading Project for Realization of Regenerative Medicine from the Ministry of Education, Culture, Sports, Science and Technology (MEXT) of Japan; Japan Science and Technology Agency (SORST); the Ministry of Health, Labor, and Welfare (to H. O.); the General Insurance Association of Japan (to M.N. and Y.T; this is not a commercial entity); Research Fellowships for Young Scientists from the Japan Society for the Promotion of Science (to Y. O.); Keio Gijuku Academic Development Funds; and by a Grant-in-aid for Global COE Program from MEXT to Keio University. The funders had no role in study design, data collection and analysis, decision to publish, or preparation of the manuscript.

Competing Interests: The authors have declared that no competing interests exist.

* E-mail: hidokano@sc.itc.keio.ac.jp (HO); masa@sc.itc.keio.ac.jp (MN)

Introduction

Because the adult central nervous system (CNS) has limited potential for regeneration, spinal cord injury (SCI) results in severe dysfunction, such as paraplegia and tetraplegia. With the aim of regenerating the injured spinal cord, various intraspinal cellular transplants have been investigated, especially in the sub-acute phase after injury. This period, between the acute and chronic phases, is marked by the minimal expression of cytokines, and is likely to be amenable to transplantation therapy [1,2,3,4,5]. Embryonic stem (ES) cells, with their indefinite replication potential, pluripotency, and genetic flexibility, have attracted great interest, and methods for inducing their neural differentiation have been extensively studied [6]. ES cell-derived neural progenitors are currently one of the most promising cell sources for cell transplantation therapy for treating SCI. Although previous studies demonstrated that the transplantation of mouse ES cell-derived embryoid bodies [7] or human ES cell-derived oligodendrocyte progenitor cells [8] promotes overall functional recovery after SCI, the types of neural progenitor cells most effective for treating sub-acute phase SCI has been uncertain.

We recently reported that a low concentration of retinoic acid (10^{-8} M: low-RA) can efficiently induce caudalized neural progenitors in embryoid bodies (EBs) [9], and we established a neurosphere-based culture system of ES cell-derived neural stem/progenitor cells (NS/PCs) from low-RA-treated EBs, with midbrain to hindbrain identities [10]. These ES cell-derived primary neurospheres (PNS) mainly exhibit neurogenic differentiation potentials, whereas passaged secondary neurospheres (SNS) are more gliogenic, corresponding to changes in CNS development, in which neurogenic NS/PCs predominate early in gestation and gliogenic NS/PCs predominate in mid-to-late gestation. Here, taking advantage of this difference between neurogenic PNS and gliogenic SNS, we transplanted PNS and SNS into the injured spinal cord, examined the differentiation and growth properties of the grafted cells, and compared their effects on angiogenesis, axonal regeneration, and functional recovery after SCI. We also examined the survival and growth of the

transplanted ES cell-derived NS/PCs using *in vivo*, live, bioluminescent imaging (BLI) to evaluate the tumorigenicity and safety of the grafted cells.

Results

Establishment of a Stable ES Cell Line Expressing CBR*luc* Luminescence and Venus Fluorescence

We first established an ES cell line that constitutively expresses the click beetle red-emitting luciferase (CBR*luc*) [11] and Venus [12] by introducing a CAG-CBR*luc*-IRES-Venus plasmid (Fig. 1**A**) into EB3 ES cells (CCV-ES cells) [13]. CCV-ES cells and their progenies were detected by both BLI [3,14,15] and fluorescence microscopy. To induce NS/PCs from ES cells and obtain PNS and SNS, we used a neurosphere-based culture system that we recently reported [10] (Fig. 1**B**), as described in Materials and Methods. More than 99% of the undifferentiated CCV-ES cells expressed Venus fluorescence by flow cytometry (Fig. 1**D and E**), and CCV-ES cell-derived PNS (CCV-PNS) and SNS (CCV-SNS) showed steady fluorescence that was detectable by fluorescence microscopy (Fig. 1**C**). Approximately 80% of the cells in the CCV-PNS and -SNS were positive for Venus by flow cytometry (Fig. 1**D and E**). bioluminescence imaging (BLI) revealed CBR*luc* expression in both CCV-PNS and –SNS, and we confirmed that the photon counts were in direct proportion to the cell numbers *in vitro* (Fig. 1**F**). We also confirmed that the CCV-ES cells could generate PNS and SNS similar to EB3-ES cells (Fig. 1**C**).

Distinct Differentiation Potentials of PNS and SNS *In Vitro*

We next examined the *in vitro* differentiation potentials of the PNS and SNS derived from EB3- and CCV-ES cells. PNS and SNS derived from EB3- and CCV-ES cells were allowed to differentiate in medium without FGF2 on poly-L-ornithine/fibronectin coated coverslips for 5 days, and then processed for immunocytochemistry. We examined the frequency of colonies consisting of βIII tubulin-positive neurons, GFAP-positive astrocytes, and/or O4-positive oligodendrocytes, and found that the EB3- and CCV-PNS colonies predominantly differentiated into neurons, although a small number of colonies contained both neurons and glia (Fig. 1**G**). In contrast, most of the EB3- and CCV-SNS colonies differentiated into both neurons and glia, including astrocytes and oligodendrocytes, or into only glial cells (Fig. 1**G**), demonstrating that the ES cell-derived PNS and SNS had distinct differentiation potentials *in vitro* (Fig. 1**H**). Moreover, EB3- and CCV-ES cell-derived neurospheres exhibited similar differentiation properties, confirming that the transgene in the ES cells had negligible effects on differentiation (Fig. 1**H**).

We also examined the SNS formation rates to determine the self-renewing ability of the ES cell-derived PNS. We cultured CCV-PNS at a low cell density (2.5×10^4 cells/ml), transferred them into 96-well plates at one neurosphere/well, dissociated the neurospheres, and cultured them again with FGF2 to form secondary neurospheres. Most of the CCV-PNS generated secondary neurospheres (79/90; 87.7%; from more than three independent experiments), confirming their ability to self-renew.

Transplanted SNS Prevented Atrophic Change and Demyelination after SCI

A contusive SCI was induced at the Th10 level of C57BL6 mice, and 5×10^5 cells of CCV-PNS or CCV-SNS, or PBS as a control, were injected into the lesion epicenter 9 days after injury. We refer to these, respectively, as the PNS, SNS, and control groups. After 6 weeks, histological analyses were performed. We first examined atrophic changes of the injured spinal cord by Hematoxylin-eosin (H–E) staining (Fig. 2**A and B**). The transverse area of the spinal cord at the lesion epicenter was significantly larger in the SNS group than in the control group, suggesting that SNS transplantation prevented atrophy of the injured spinal cord (Fig. 2**E**). Luxol Fast Blue (LFB) staining revealed significantly greater preservation of the myelinated areas in the SNS group compared with the control (both 2 and 6 weeks after injury) and PNS groups (Fig. 2**C and D**), from 1 mm rostral to 1 mm caudal to the epicenter (Fig. 2F). Notably, there was a significantly spared rim of white matter in the SNS group, even at the lesion epicenter, whereas the control group exhibited severely demyelinated white matter throughout the lesioned area (2 mm rostral and caudal to the lesion epicenter) (Fig. 2**C and D**).

Transplanted PNS and SNS survived in the injured spinal cord and did not form tumors

The photon count measured by bioluminescence imaging (BLI) quantifies only living cells, since the luciferin-CBR-luciferase reaction depends on oxygen and ATP. The successful transplantation of CCV-PNS and -SNS was confirmed immediately after transplantation using BLI, and the average signal intensity was $2.2\pm1.6\times10^5$ photons/mouse/sec in 22 transplanted mice. Images obtained weekly thereafter for 6 weeks showed that the signal intensity dropped sharply within the first week after transplantation, but remained at 20% of the initial photon count in both the PNS and SNS transplantation groups throughout the remaining period. Although the signal intensity at 1 week was significantly higher in the PNS group (62.4%) than in the SNS group (29.5%), there was no significant difference in the signal intensity between the PNS (12.6%) and SNS (18.9%) groups at 6 weeks, suggesting there was a similar number of live grafted PNS- and SNS-derived cells within the injured spinal cord 6 weeks after transplantation. Thus, similar numbers of grafted PNS and SNS cells may have survived in the injured spinal cord, although the possibility that the grafted cells proliferated differently in the two groups 1 to 6 weeks after transplantation cannot be excluded. Notably, a rapid increase in signal intensity, which would have suggested tumor formation, was not observed during this time period (Fig. 3**A and B**). Consistently, histological analysis confirmed that both the CCV-PNS- and CCV-SNS-derived Venus-positive cells survived without forming tumors (Fig. 3**C–F**). Quantitative analysis of the Venus-positive area revealed that there was no significant difference of the number of survived grafted cells between PNS and SNS groups 6 weeks after transplantation (Fig. 3**G**). Moreover, the data of BLI correlated well with Venus-positive area (Pearson's correlation coefficient: 0.759, $p=0.04$, Fig. 3**H**).

PNS and SNS Grafted onto Injured Spinal Cord Exhibited Differentiation Potentials Similar to Those Observed *In Vitro*

To examine the differentiation characteristics of CCV-PNS and -SNS grafted onto the injured spinal cord, we performed immunohistochemical analyses, and determined the proportion of cells immunopositive for each cell type-specific marker among the Venus-positive grafted cells [3]. Both the PNS- and SNS-derived cells integrated at or near the lesion epicenter and differentiated into Hu-positive neurons, GFAP-positive astrocytes, and APC-positive oligodendrocytes (Fig. 4**A–E**). The percentage of Hu/Venus double-positive neurons in the PNS group ($52.8\pm19.1\%$) was three times that in the SNS group ($16.3\pm5.2\%$) (Fig. 4**F**). In contrast, the percentage of GFAP/Venus double-positive astrocytes or APC/Venus double-positive

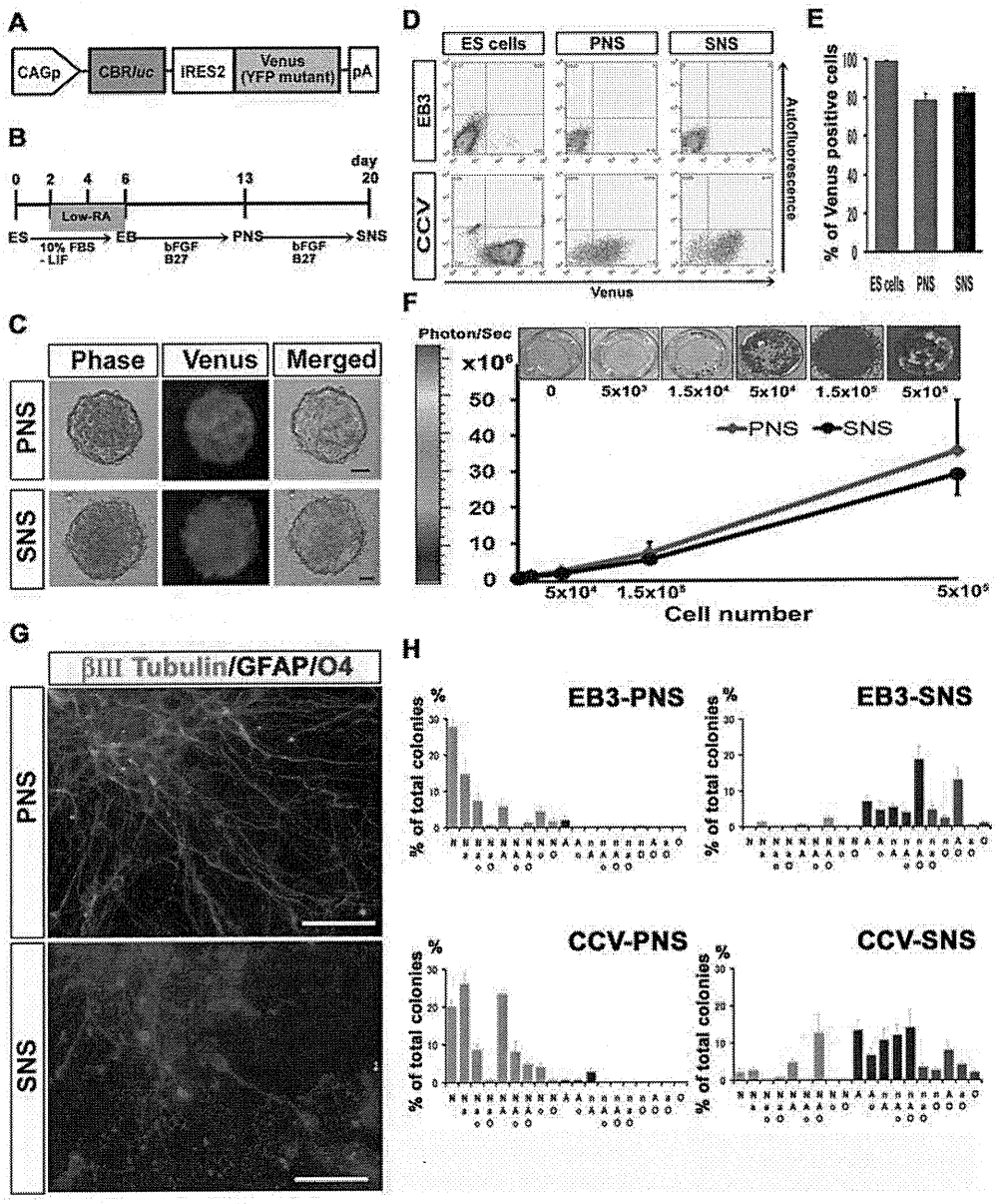

Figure 1. Establishment of a stable ES cell line expressing CBR/*luc* luminescence and Venus fluorescence, and their differentiation analysis. (A) The CAG-CBR/*luc*–IRES-Venus gene (CCV) construct. (B) Protocols for deriving neurospheres from mouse ES cells. ES cells were dissociated into single cells with 0.25% trypsin-EDTA and cultured for 6 days to allow the formation of embryoid bodies (EBs). A low concentration of RA was added on day 2 of EB formation for neural induction. The EBs were dissociated into single cells with 0.25% trypsin-EDTA and cultured in suspension for 7 days, to obtain primary neurospheres (ES cell-derived primary neurospheres, PNS). These PNS were dissociated into single cells with TripleLE Select (Invitrogen) and cultured again in suspension for 7 days under the same conditions to form secondary neurospheres (SNS). (C) Images of CCV-PNS and -SNS visualized by fluorescence microscopy. Scale bar: 100 μm. (D) Flow cytometric analysis of Venus-positive cells in PNS and SNS derived from CCV- and EB3-ES cells. (E) The proportion of Venus-positive cells among CCV-ES cells and their progenies, CCV-PNS and -SNS. Approximately 80% of the CCV-PNS and -SNS cells were positive for Venus. Values are means ± s.e.m. ($n = 3$). (F) Correlation between the cell numbers of CCV-PNS and -SNS, and the measured photon counts. BLI revealed CBR*luc* expression in both CCV-PNS and -SNS, and we determined that the photon counts were in direct proportion to the cell numbers *in vitro*. Values are means ± s.e.m. ($n = 3$). (G)(H) Distinct differentiation potentials of PNS and SNS *in vitro*. Immunocytochemical analysis of βIII tubulin-positive neurons (N or n), GFAP-positive astrocytes (A or a), and O4-positive oligodendrocytes (O or o) (N, A, O: more than 20 cells; n, a, o: fewer than 19 cells in each colony, respectively). A neuron-only colony (N) and a colony consisting of astrocytes and oligodendrocytes (AO) are shown (G). Scale bar: 50 μm. Quantitative analysis of the *in vitro* differentiation potential of EB3-PNS and -SNS and CCV-PNS and -SNS, shown as the percentage of each phenotypic colony among the total colonies (H). The PNS colonies dominantly differentiated into neurons, while a small number of colonies contained glial cells. On the other hand, most of the SNS colonies differentiated into both neurons and glial cells, including astrocytes and oligodendrocytes, or into only glial cells. Values are means ± s.e.m. ($n = 3$).
doi:10.1371/journal.pone.0007706.g001

oligodendrocytes in the SNS group (42.2±14.4, 33.6±5.4%) was twice that in the PNS group (19.0±9.3, 14.8±7.1%) (Fig. 4**F**) (n = 4). The differentiation patterns of the grafted PNS and SNS were consistent with the results of the *in vitro* differentiation assay, suggesting that PNS and SNS preserved their differentiation tendencies *in vivo*.

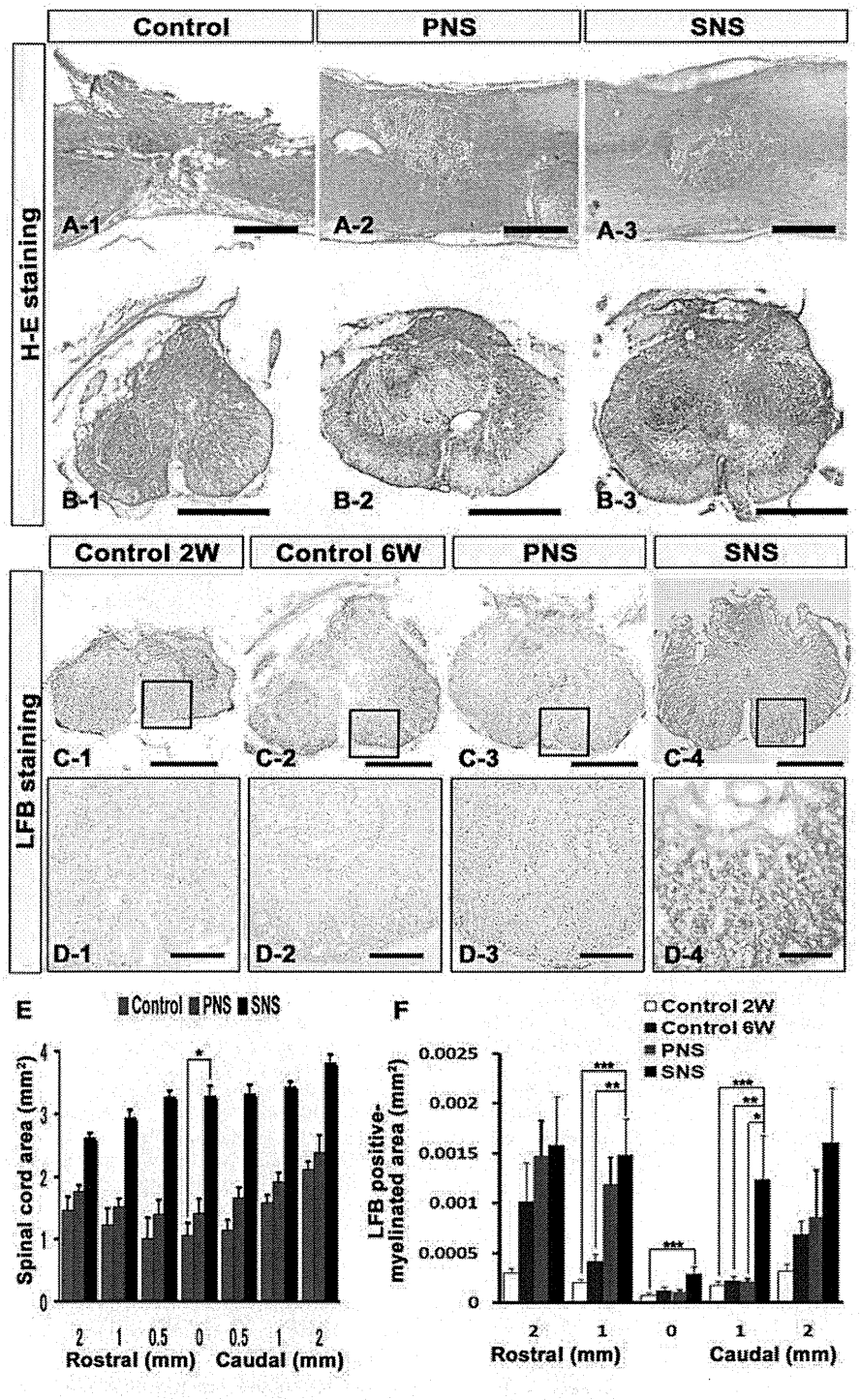

Figure 2. Transplanted SNS prevented atrophic change and demyelination after SCI. (A)(B) Representative H–E staining images of the sagittally sectioned (A1–3) and axially sectioned (B1–3) spinal cord at the lesion epicenter 6 weeks after injury. Scale bar: 500 μm. (C) Representative LFB staining images of the axially sectioned spinal cord 1 mm caudal to the lesion from each animal (2 weeks or 6 weeks after SCI for the vehicle-control group and 6 weeks after SCI for the PNS and SNS groups). Scale bar: 500 μm. (D) Higher magnification images of the boxed areas in C. Scale bar: 100 μm. (E) Quantitative analysis of the spinal cord area measured in H–E-stained axial sections through different regions. The transverse area of the spinal cord at the lesion epicenter was significantly larger in the SNS group compared with the control group. Values are means ± s.e.m. ($n = 5$). *: $P<0.05$, Control vs. SNS. (F) Quantitative analysis of the myelinated area by LFB-stained axial sections at different regions. LFB staining revealed greater preservation of myelination in the SNS group, with significant differences observed at the sites 1 mm rostral and 1 mm caudal to the epicenter compared with the control 2 or 6 weeks groups, 1 mm caudal to the epicenter compared with the PNS group, and at the epicenter compared with the control 2-week group. Values are means ± s.e.m. ($n = 5$). *: $P<0.05$, PNS vs. SNS. **: $P<0.05$, Control 6 weeks vs. SNS. ***: $P<0.05$, Control 2 weeks vs. SNS.

doi:10.1371/journal.pone.0007706.g002

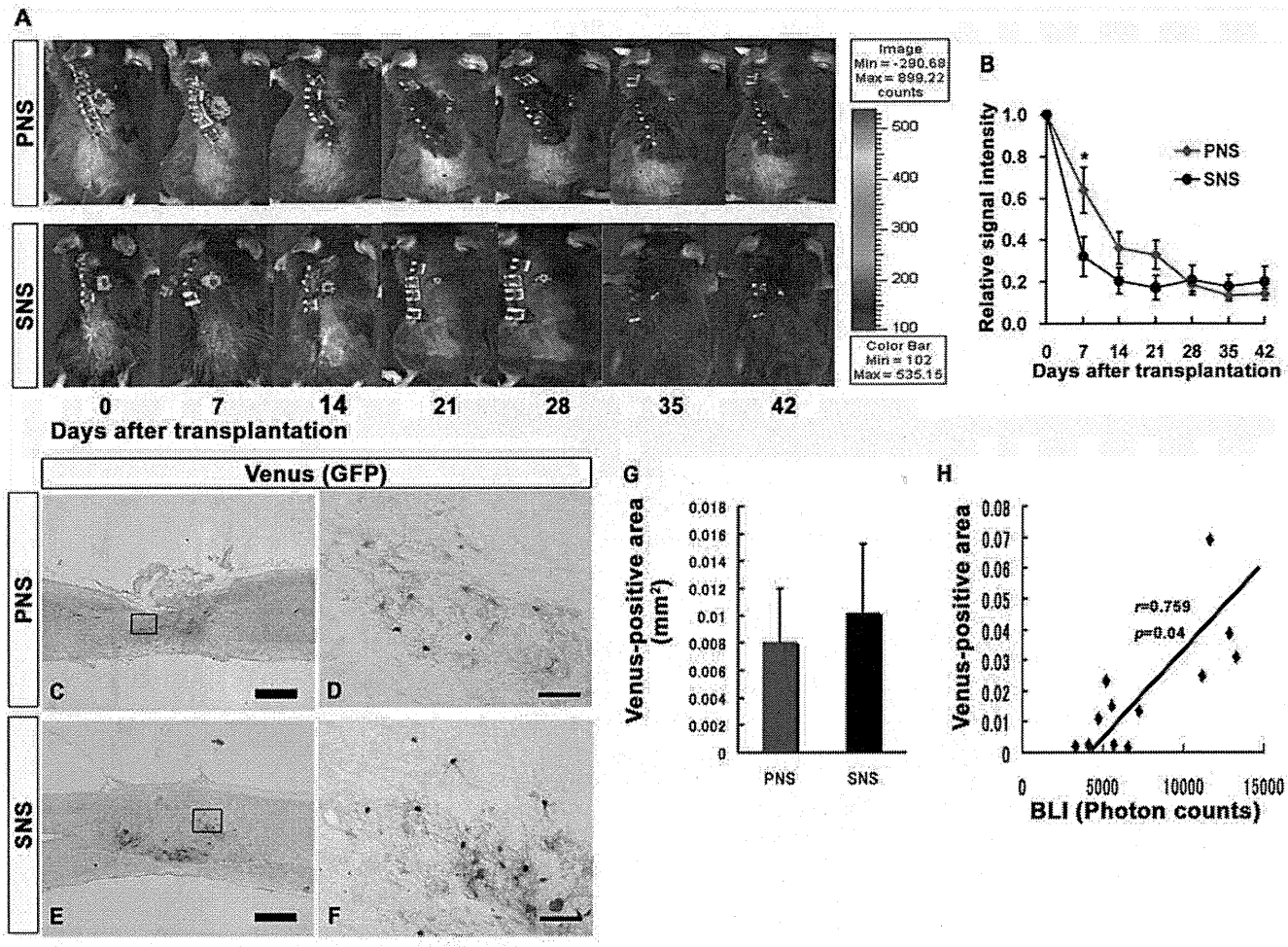

Figure 3. Transplanted PNS and SNS survived in the injured spinal cord and did not form tumors. (A) Representative BLI images of mice that received transplants of CCV-PNS and -SNS. (B) Signal intensity over time after transplantation in the PNS and SNS groups, shown relative to the initial value. Although the signal intensity at 1 week after the injury was significantly higher in the PNS group (62.4%) than the SNS group (29.5%), there was no significant difference in the signal intensity between the PNS (12.6%) and SNS (18.9%) groups 6 weeks after the injury. Values are means ± s.e.m. ($n = 11$). *: $P<0.05$, PNS vs. SNS. Scale bar: 500 μm. (C)(D)(E)(F) Representative images of sagittal sections of spinal cords grafted with PNS and SNS, which were immunostained for Venus (grafted cells) using an anti-GFP antibody. High-magnification images of the boxed areas in C and E are shown in D and F. Scale bar: 500 μm for C and E, 100 μm for D and F. Histological analysis confirmed that both PNS- and SNS-derived cells survived without forming tumors. (G) Quantitative analysis of Venus (GFP)-positive area at the lesion epicenter in midsagittal sections. Venus immunostaining revealed there was no significant difference between PNS and SNS groups 6 weeks after transplantation Values are means ± s.e.m. (n = 6). (H) Correlation of the results of BLI analysis and the quantification of Venus-positive area. The data of BLI correlated well with Venus-positive area (n = 12).

doi:10.1371/journal.pone.0007706.g003

Transplanted SNS, but Not PNS, Enhanced Angiogenesis after SCI

To examine the effects of CCV-PNS and -SNS transplantation on angiogenesis after SCI, sagittal and axial sections of the injured spinal cord were examined immunohistochemically for αSMA (a marker for smooth muscle cells) or PECAM-1 (a marker for endothelial cells). While a few αSMA-positive cells were observed at and near the lesion site in sagittal sections of both the control and PNS groups, significantly more αSMA-positive cells were found in the SNS group (Fig. 5**A and B**). These αSMA-positive cells accumulated near Venus-positive grafted cells (Fig. 5**C and D**). Similarly, significantly more PECAM-1-positive blood vessels were observed at the lesion site in the SNS group than in the PNS and control groups (Fig. 5**E–J, Y**). To clarify the underlying angiogenic signals, we examined the expression of an angiogenic growth factor, vascular endothelial growth factor (VEGF), in the grafted spinal cord by immunohistochemistry. Although a VEGF-positive area was observed at the lesion epicenter in all three groups 6 weeks after injury (Fig. 5**K–M**), it was significantly broader in the SNS group than in the other groups (Fig. 5**Z**). Furthermore, we found many GFAP/VEGF double-positive host astrocytes, which were negative for Venus (GFP) (Fig. 5**N–Q**), and a few Venus (GFP)/GFAP-positive graft-derived astrocytes expressing VEGF (Fig. 5**R–X**).

Transplanted SNS, but Not PNS, Promoted Axonal Regrowth and Enhanced Functional Recovery

To examine the effects of CCV-PNS and -SNS transplantation on axonal regrowth after SCI, we performed immunohistochemical analyses of the injured spinal cord for NF-H (RT97), 5-hydroxytryptamine (5-HT), and growth-associated protein-43 (GAP43). While few NF-H-positive axons were observed at the